Petrogenetic links between lepidolite-subtype aplite-pegmatite, aplite veins and associated granites at Segura (central Portugal)

Article *in* Chemie der Erde - Geochemistry · October 2013

DOI: 10.1016/j.chemer.2012.12.003

Margarida HR Antunes
University of Minho

Ana. M. R. Neiva
University of Coimbra

João Manuel farinha Ramos
Laboratório Nacional de Energia e Geologia

Paulo Bravo Silva

Chemie der Erde 73 (2013) 323–341

Contents lists available at ScienceDirect

Chemie der Erde

journal homepage: www.elsevier.de/chemer

Petrogenetic links between lepidolite-subtype aplite-pegmatite, aplite veins and associated granites at Segura (central Portugal)

Isabel Margarida Horta Ribeiro Antunes[a,*], Ana Margarida Ribeiro Neiva[b], João Manuel Farinha Ramos[c], Paulo Bravo Silva[c], Maria Manuela Vinha Guerreiro Silva[b], Fernando Corfu[d]

[a] Polytechnic Institute of Castelo Branco, 6001-909 Castelo Branco, Portugal
[b] Department of Earth Sciences and Geosciences Centre, University of Coimbra, 3000-272 Coimbra, Portugal
[c] LNEG National Laboratory of Energy and Geology, Apartado 1089, 4466-956 S. Mamede de Infesta, Portugal
[d] Department of Geosciences, University of Oslo, PB1047, Blindern N-0316, Norway

ARTICLE INFO

Article history:
Received 18 July 2012
Accepted 29 December 2012

Keywords:
Aplites
Lepidolite-subtype aplite-pegmatites
Lepidolite
Montebrasite
Sn–Nb–Ta oxide minerals
Parent granite
Crystal fractionation

ABSTRACT

In the Segura area, Variscan S-type granites, aplite veins and lepidolite-subtype granitic aplite-pegmatite veins intruded the Cambrian schist-metagraywacke complex. The granites are syn D3. Aplite veins also intruded the granites. Two-mica granite and muscovite granite have similar ages of 311.0 ± 0.5 Ma and 312.9 ± 2.0 Ma but are not genetically related, as indicated by their geochemical characteristics and $(^{87}Sr/^{86}Sr)_{311}$ values. They correspond to distinct pulses of magma derived by partial melting of heterogeneous metapelitic rocks. Major and trace elements suggest fractionation trends for: (a) muscovite granite and aplite veins; (b) two-mica granite and lepidolite-subtype aplite-pegmatite veins, but with a gap in most of these trends. Least square analysis for major elements, and modeling of trace elements, indicate that the aplite veins were derived from the muscovite granite magma by fractional crystallization of quartz, plagioclase, K-feldspar and ilmenite. This is supported by the similar $(^{87}Sr/^{86}Sr)_{311}$ and $\delta^{18}O$ values and the behavior of P_2O_5 in K-feldspar and albite. The decrease in $(^{87}Sr/^{86}Sr)_{311}$ and strong increase (1.6‰) in $\delta^{18}O$ from two-mica granite to lepidolite-subtype aplite-pegmatite veins, and the behaviors of Ca, Mn and F of hydroxylapatite indicate that these veins are not related to the two-mica granite.

The occurrence of amblygonite–montebrasite, lepidolite, cassiterite, columbite-(Fe), columbite-(Mn) and microlite suggests that lepidolite-subtype granitic aplite-pegmatite veins are highly differentiated. Montebrasite shows a heterogeneous Na distribution and secondary lacroixite was identified in some montebrasite areas enriched in Na. Unusual Mn > Fe cassiterite is zoned, with the alternating darker zones being strongly pleochroic, oscillatory zoned, and containing more Nb and Ta than the lighter zones. Inclusions of muscovite, apatite, tapiolite-(Fe), ixiolite and microlite are present both in lighter and darker zones of cassiterite. It shows exsolutions of columbite-(Fe), columbite-(Mn,Fe) and columbite-(Mn), particularly in darker zones.

1. Introduction

The mineralization processes related to granites, pegmatites and hydrothermal veins involve the enrichment of rare elements (e.g., Be, Ta, Li, Sn, Bi, W, Mo, Cu) and volatiles in late residual magma, or their enrichment in volatile phases in the final stages of magmatic crystallization (Beurlen et al., 2001). Almost all rare-element pegmatite types (low temperature and pressure) are associated with highly fractionated peraluminous granites (Černý, 1992) and are accepted as the products of magmatic differentiation from large granite bodies (e.g., Černý, 1992; Leal Gomes, 2006; Neiva et al., 2008, 2012; Neiva and Ramos, 2010). However, this mechanism is difficult to test for pegmatites (e.g., Neiva et al., 2008, 2012; Neiva and Ramos, 2010), due to the presence of B, F, P and Li fluxes, which are involved in the crystallization of tourmaline, topaz, montebrasite–amblygonite, lepidolite, and influence the crystallization of cassiterite, columbite-tantalite and microlite (e.g., Linnen and Cuney, 2005). These pegmatite minerals are important indicators, as the origin of the pegmatites must be responsible for the occurrence of all their minerals. Some examples of lepidolite-subtype pegmatites do not show this mineral association, as the volatile-rich fluids are stable at relatively low temperatures and commonly migrate to great distances from their plutonic sources (Černý et al., 2005). Therefore, parent granite and pegmatites can be spatially separated (e.g., Currie et al., 1998).

The aplite-pegmatite veins from Segura are REL-Li pegmatites and belong to the LCT family (sensu Černý and Ercit, 2005), which is characterized by the enrichment in Li, Cs and Ta. In central Portugal,

* Corresponding author. Tel.: +351 964219682; fax: +351 272339901.
E-mail address: imantunes@ipcb.pt (I.M.H.R. Antunes).

0009-2819/$ – see front matter © 2013 Elsevier GmbH. All rights reserved.
http://dx.doi.org/10.1016/j.chemer.2012.12.003

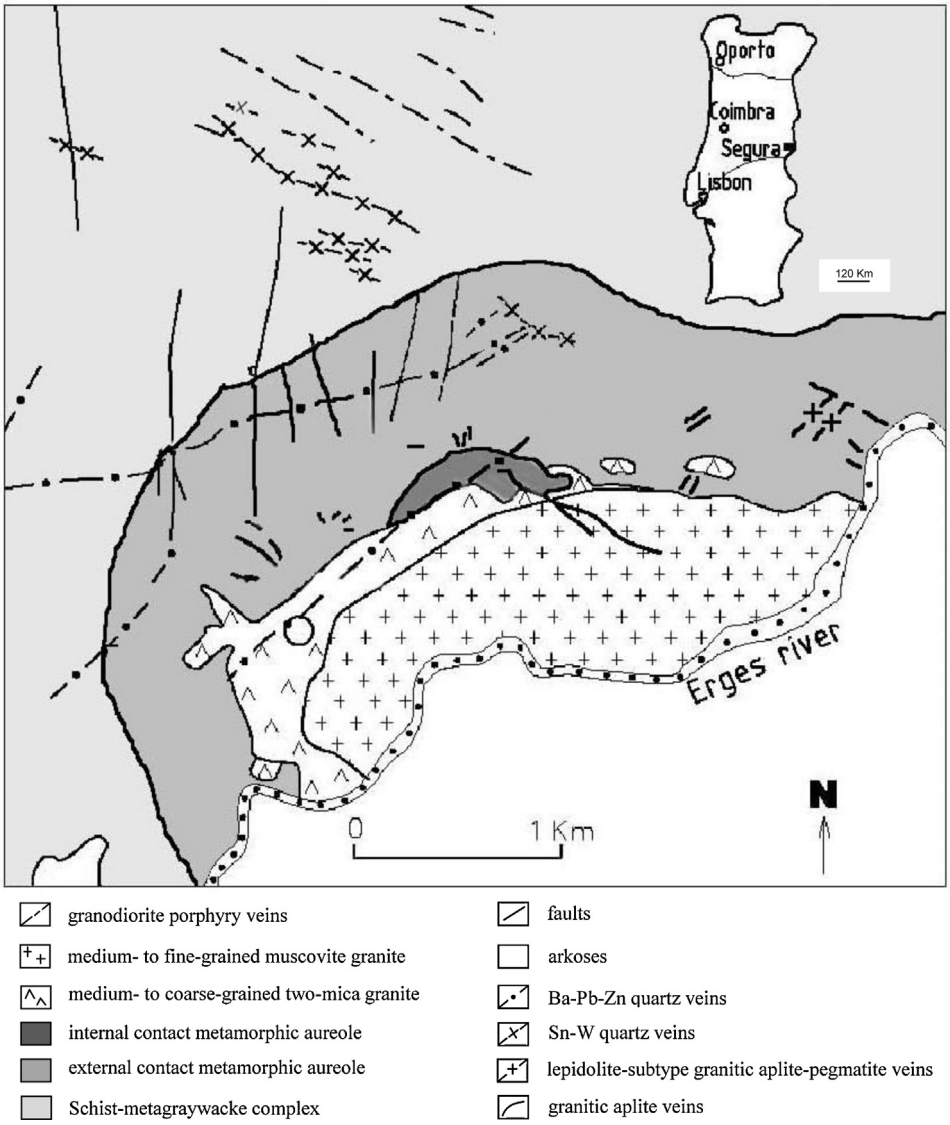

Fig. 1. Geological map of Segura, central Portugal.

there is an extensive field of LCT granitic aplite-pegmatite veins. They are mostly linked to S-type, peraluminous granitic rocks that were emplaced during the last deformation phase of the Variscan Orogeny (D3) and, therefore, are classified as syn- to post-D3 granites (e.g., Dias et al., 1998; Ramos et al., 2006; Cotelo Neiva, 2006). The mineralogy and geochemistry of lepidolite-subtype granitic aplite-pegmatite veins and associated granites and aplite veins from Segura are presented here and the data are used to discuss their origin and petrogenetic models.

2. Geological setting

The Segura area, located in central Portugal, close to the Portuguese–Spanish border (Fig. 1), is part of the Iberian Massif, which corresponds to the SW extension of the European Variscan Belt. It also belongs to the Central Iberian Pegmatitic Belt (Leal Gomes, 2006). The syn-D3 Variscan pluton of Segura intruded the schist-metagraywacke complex, which consists of alternating metapelites and metagraywackes with metaconglomerate and marble intercalations, initially deposited in Cambrian times. The contact metamorphic aureole is up to 500 m thick, with an outer zone of mica schist containing cordierite porphyroblasts and an inner zone with hornfels, containing cordierite and sillimanite, up to 20 m thick (Fig. 1).

The Segura pluton is exposed over an area of about 4 km^2 and is dominated by a medium- to coarse-grained two-mica granite, but a medium- to fine-grained muscovite-bearing granite also intruded the schist-metagraywacke complex (Fig. 1). The contact between these granites is sharp (Antunes et al., 2009). Subvertical, N45-60W trending veins of granodiorite porphyry intruded the schist-metagraywacke complex in the northern part of the area. Other crosscutting vein systems include NW-SE to NNW-SSE trending granitic aplite veins, subhorizontal NE-SW trending lepidolite-subtype, granitic aplite-pegmatite veins containing cassiterite and lepidolite (Fig. 2a), NW-SE to WNW-ESE trending quartz veins containing cassiterite and wolframite and ENE-WSW to NNE-SSW trending quartz veins containing barite, galena and sphalerite (Fig. 1). One of the latter veins also cuts the muscovite granite. These veins are up to 15 cm thick and 300 m long (Antunes et al., 2002).

The mineralized quartz veins fill late- to post-tectonic Variscan faults. Nowadays it is difficult to recognize the mineralized veins, because they generally occur in the old mines, which were in operation from 1949 to 1953.

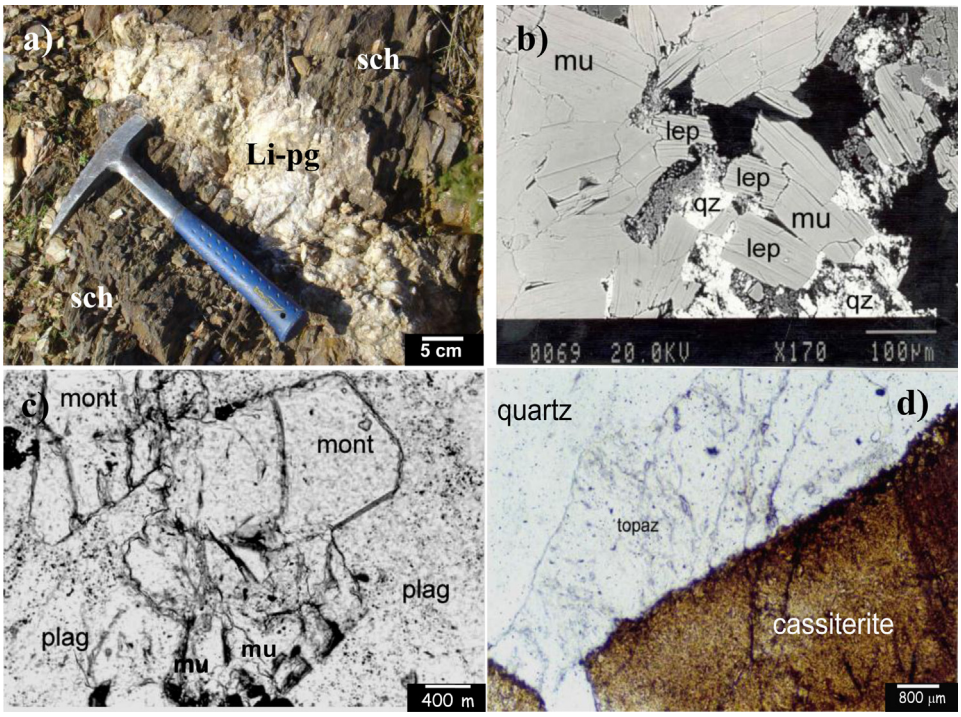

Fig. 2. Textural characteristics of lepidolite-subtype granitic aplite-pegmatite veins of Segura. (a) Lepidolite-subtype granitic aplite-pegmatite veins (Li-pg) cutting the schist-metagraywacke complex (sch); (b) lepidolite (lep) partially replacing muscovite (mu) with quartz (qz); (c) subhedral montebrasite (mont) replaced by muscovite (mu) with associated plagioclase (plag); (d) topaz associated with quartz and cassiterite.

3. Petrography

The granitic rocks from Segura contain quartz, microperthitic microcline, albite, muscovite, apatite, zircon, monazite, rutile and ilmenite. The two-mica granite also has biotite, chlorite (after biotite), sillimanite and tourmaline and the aplite veins also have tourmaline. The muscovite granite contains secondary gormanite (Antunes et al., 2009). The granites display a subhedral granular microstructure, whereas the two-mica granite also presents a seriate microstructure. The lepidolite-subtype aplite-pegmatite veins also contain frequent amblygonite–montebrasite, topaz, lepidolite, cassiterite, tapiolite, columbite, ixiolite and microlite. Secondary lacroixite was found associated with montebrasite. The pegmatites belong to the LCT family, rare-element class (REL), REL-Li subclass, complex type and lepidolite-subtype (Černý and Ercit, 2005).

Quartz is euhedral to subhedral, shows undulose extinction and has multiple fractures. There are different generations of quartz. The last quartz generation occurs along microcline and albite fractures. Microperthitic microcline with cross-hatch twinning is subhedral to anhedral and is locally associated with tourmaline and replaced by later secondary muscovite. Subhedral orthoclase crystals were found in muscovite granite. Subhedral plagioclase is albite with compositions of An_0–An_5 in two-mica granite, An_0–An_1 in muscovite granite, An_0–An_3 in aplite veins and An_0–An_1 in lepidolite-subtype granitic aplite-pegmatite veins (Antunes et al., 2009).

Biotite from two-mica granite is subhedral and pleochroic with γ, β (dark reddish brown) > α (pale yellow). It contains inclusions of apatite and zircon. Chlorite replacing biotite is pleochroic with γ, β (dark green) > α (light green). Primary muscovite is also subhedral, it occurs in all granitic rocks and contains inclusions of quartz, zircon and apatite. Primary muscovite from aplite veins is euhedral or radial and locally presents undulose extinction and deformed cleavage planes. Associated muscovite and lepidolite from lepidolite-subtype granitic aplite-pegmatite veins are subhedral; lepidolite partially replaces muscovite (Fig. 2b). Muscovite contains inclusions of zircon, apatite and quartz.

Subhedral tourmaline occurs in two-mica granite (4 mm × 2 mm in size) and aplite veins (1 mm × 1 mm in size), is pleochroic with ω (green) > ε (light green) or ω (yellowish brown) > ε (light yellow), contains inclusions of zircon and replaces mica. Fluorapatite and hydroxylapatite are euhedral to subhedral and occur in most granitic rocks. Secondary gormanite forms anhedral crystals with average dimensions of 500 µm × 100 µm in muscovite granite. It is pleochroic with Y (blue) > X ≈ Z (colorless) and is surrounded by quartz.

Subhedral montebrasite, 3 mm × 2 mm in size, from lepidolite-subtype aplite-pegmatite veins is replaced by muscovite (Fig. 2c) and shows Na-enriched zones identified as secondary lacroixite. There are many fractured crystals of topaz associated with quartz, plagioclase and locally with cassiterite (Fig. 2d). Topaz contains inclusions of albite.

Euhedral crystals of cassiterite ranging from 6.2 mm × 2.1 mm to 18 mm × 5.6 mm in size, either form unzoned brownish crystals or exhibit narrow, parallel lighter and darker growth-zones (Fig. 3a and b). The darker zones are strongly pleochroic with ε (reddish brown) > ω (colorless), whereas the lighter zones are colorless (Fig. 3a). Cassiterite contains inclusions of muscovite and apatite. Subhedral to euhedral zoned inclusions of tapiolite-(Fe) (40 µm × 30 µm), ixiolite (30 µm × 15 µm) and microlite (80 µm × 30 µm) were also found in cassiterite (Fig. 3c–g). Cassiterite shows subhedral zoned tapiolite-(Fe), columbite-(Fe), columbite-(Mn,Fe) and columbite-(Mn) exsolutions of 300 µm × 600 µm (Fig. 3d–g). Some zoned crystals range from columbite-(Fe) to columbite-(Mn) (Fig. 3h).

4. Analytical methods

Lepidolite from lepidolite-subtype aplite-pegmatite veins was separated using a magnetic separator and heavy liquids. A purity

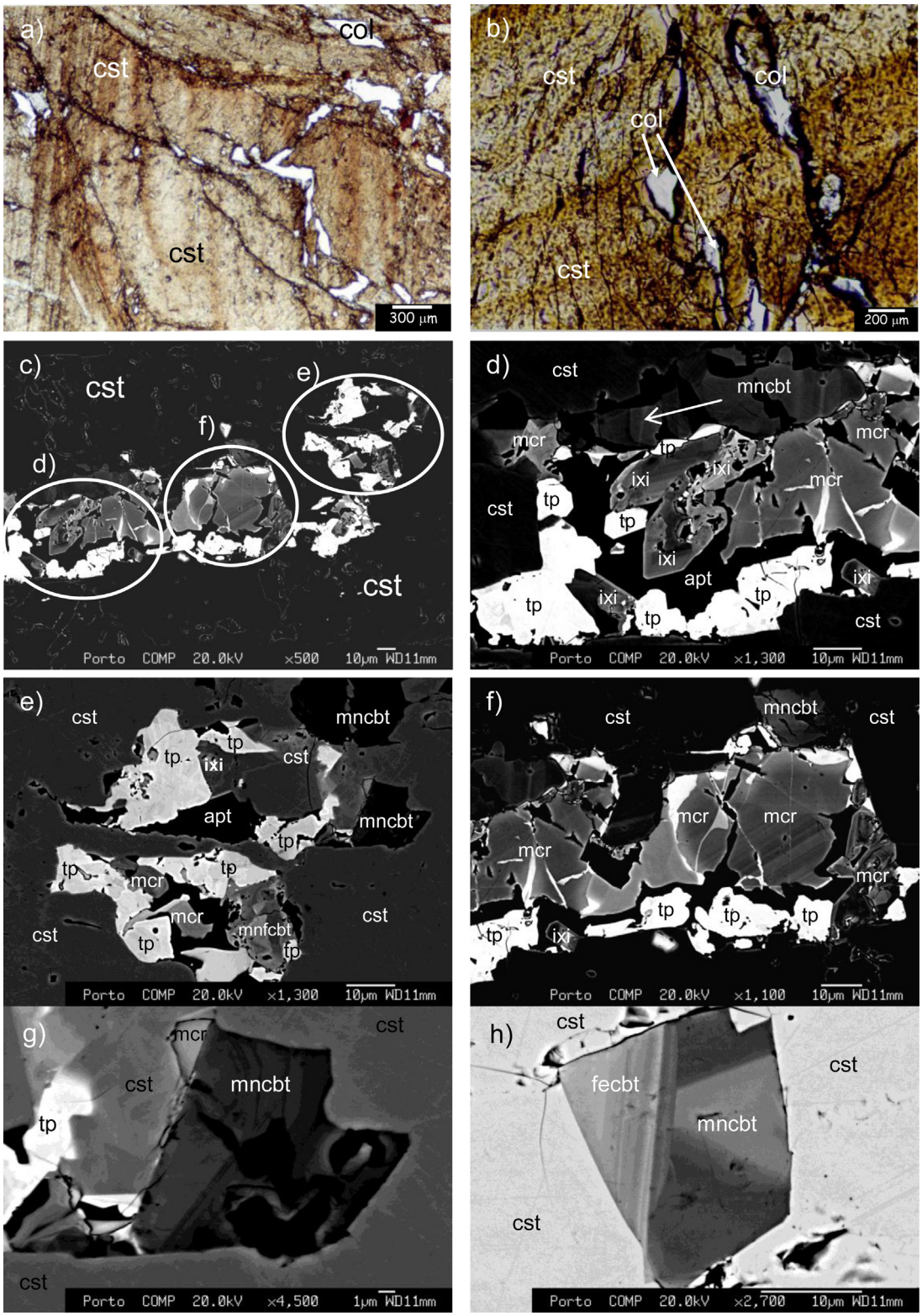

Fig. 3. Cassiterite with inclusions and exsolution products from lepidolite-subtype granitic aplite-pegmatite veins. Microphotographs: (a) lighter and darker growth-zones of cassiterite (cst) with exsolved columbite-group minerals (col); (b) subhedral columbite-group mineral (col) exsolved from a cassiterite crystal (cst). Backscattered electron images: (c) zoned cassiterite (cst) with inclusions and exsolution products showing the location of areas amplified in the pictures (d–f); (d) zoned cassiterite (cst) with inclusions of apatite (apt), ixiolite (ixi), tapiolite-(Fe) (tp) and microlite (mcr) and a columbite-(Mn) (mncbt) exsolution; (e) cassiterite (cst) with tapiolite-(Fe) (tp) in the border zone, inclusions of ixiolite (ixi) and microlite (mcr) associated with subhedral columbite-(Mn) (mncbt) and columbite-(Mn,Fe) (mnfcbt) exsolutions; (f) cassiterite (cst) with inclusions of microlite (mcr) and tapiolite-(Fe) (tp) and a columbite-(Mn) (mncbt) exsolution; (g) subhedral zoned exsolution of columbite-(Mn) (mncbt), with tapiolite-(Fe) (tp) and an associated microlite (mcr) inclusion in a cassiterite (cst) crystal; (h) subhedral zoned exsolution of cassiterite (cst) showing a variation in composition from columbite-(Fe) (fecbt) to columbite-(Mn) (mncbt).

of about 99.8% was estimated by petrographic examination of the mineral separates. The principal contaminant is zircon.

Major and trace elements of granites, aplite and aplite-pegmatite veins were analyzed by X-ray fluorescence at Southampton Oceanography Centre in Southampton, UK, with a Philips Magic ProPW 2540 VRC Spectrometer, using the method of Croudace and Thorpe (1988) and Croudace and Gilligan (1990). Glass beads were used to determine major elements, whereas powder pellets were prepared to analyze trace elements. Precision is ±1% for major elements and ±5% for trace elements. The FeO content of granitic rocks was determined by titration with a standardized potassium permanganate solution and H_2O+ was analyzed using a Penfield tube, both with a precision of about ±1%. The Li content of granitic rocks and lepidolite from lepidolite-subtype aplite-pegmatite veins was determined by atomic absorption, while F was analyzed by selective ion electrode analysis, the precision being about ±2% for both. These determinations were carried out in the Department of Earth Sciences, University of Coimbra. The Li content of muscovite was calculated using the equation $Li_2O = 0.3935F^{1.326}$ of Tischendorf et al. (1997). Rare earth elements were determined by ICP-MS with an accuracy of ±5% in the SGS Laboratory, Canada.

Zircon and monazite separation was carried out by a combination of magnetic separator and heavy liquids. The grains to be analyzed were selected by handpicking under a binocular microscope. Zircon was treated with chemical abrasion (3 days annealing at 900 °C and 1 night partial dissolution at ca. 190 °C; modified from Mattinson, 2005), and monazite with air abrasion (Krogh, 1982). The U–Pb isotopic results were obtained by isotope dilution thermal ionization mass spectrometry (ID-TIMS) using a Finnigan-Mat 262 spectrometer at the Department of Geosciences, University of Oslo, Norway, following the adaptations described by Corfu and Evins (2002) and Corfu (2004). The initial Pb correction was done using compositions calculated with the Stacey and Kramers (1975) model. The decay constants used are those of Jaffey et al. (1971). The Isoplot program was used for the plots and regression (Ludwig, 2003). All uncertainties relative to the analyses and ages are given at the 2σ level.

Strontium isotope analyses in whole rock samples were determined by thermal ionization mass spectrometry (TIMS) with a Finnigan Mat 262 at the Geochronology and Isotopic Geochemistry Facility of the University of the Basque Country/EHU, Spain. The external precision (1σ) of $^{87}Sr/^{86}Sr$ was better than ±0.0015% and measurements of the standards yielded $^{87}Sr/^{86}Sr = 0.710273 \pm 0.000018$ (2σ) for NBS 987. The Rb and Sr contents were determined by XRF with accuracies of better than ±1% for Rb and ±5% for Sr at the Department of Geology, University of Oviedo, Spain. Whole rock oxygen isotope analyses were carried out at the University of Western Ontario, Canada, using a conventional extraction line and employing chlorine trifluoride as the reagent and a quartz standard, with a reproducibility of ±0.2‰.

The minerals were analyzed for major and minor elements on a Cameca Camebax electron microprobe at LNEG, Portugal and a JEOL JXA 8600 electron microprobe at the Department of Earth Sciences, University of Bristol, UK. Some mineral analyses, backscattered electron images and X-ray mapping, were also obtained on a JEOL JXA-8500F electron microprobe at LNEG, Portugal. Analyses were conducted at an accelerating voltage of 15–20 kV and a beam current of 20 nA. Each element was counted for 20 s. Detection limits (3σ above mean background) were 0.03 wt.% oxide for most components, except F (0.1 wt.%) and BaO (0.06 wt.%), with counting times of 80 s for F and BaO. ZAF corrections were applied.

5. Geochronology of granites

Dating of zircon and monazite from a representative sample of two-mica granite (sample GTM) and zircon from a sample of muscovite granite (sample GM) was carried out using the ID-TIMS U-Pb method (Table 1).

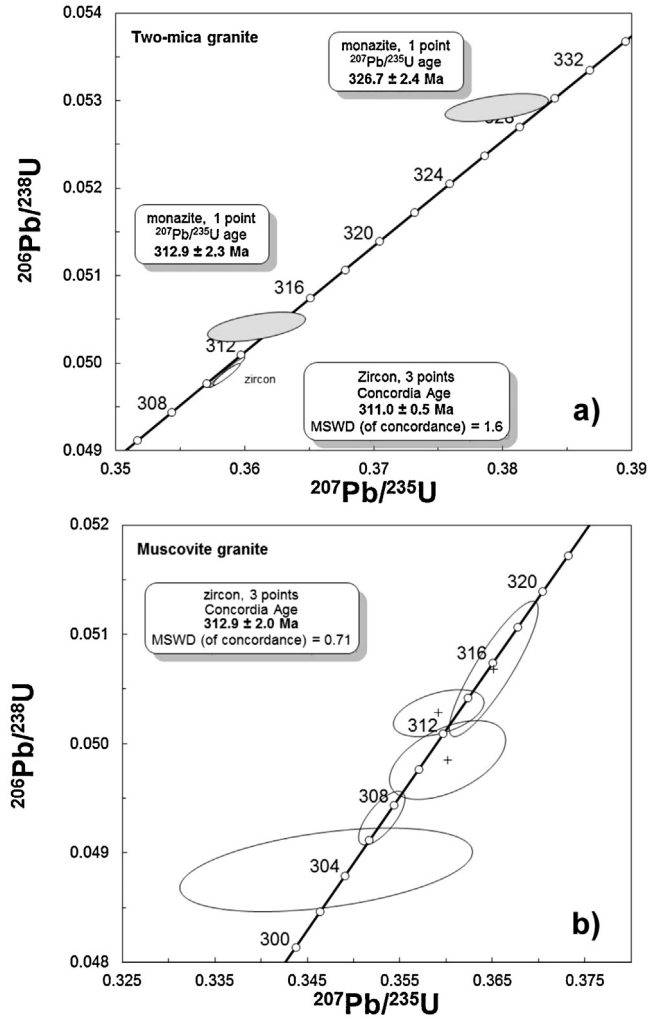

Fig. 4. Concordia diagrams displaying the U–Pb data for: (a) zircon and monazite of two-mica granite (sample # GTM); (b) zircon of muscovite granite (sample # GM). Error ellipses are drawn at 2σ.

A sample of two-mica granite contains an abundant population of elongated euhedral zircon prisms, free of cores and with prominent {2 1 1} pyramids. Three fractions of these crystals yield identical concordant data and define an age of 311.0 ± 0.5 Ma (Fig. 4a). Monazite occurs as an apparently homogeneous population of pseudo-octahedral crystals, but two analyses yield distinct ages. Both are slightly reversely discordant, a fact commonly linked to ^{206}Pb excess and reverse discordance (e.g., Schärer, 1984; Kalt et al., 2000; Antunes et al., 2008; Neiva et al., 2011). The $^{207}Pb/^{235}U$ ratio is not affected by this disequilibrium effect and can be used as the closest estimate for the age of the most concordant monazite ($^{207}Pb/^{235}U = 312.9 \pm 2.3$ Ma; Fig. 4a) overlapping the zircon age. The second monazite analysis gives an older age of 326.7 Ma, presumably reflecting an inherited component (Table 1; Fig. 4a).

The muscovite granite contains much less zircon, and most of the crystals are turbid and opaque indicating widespread metamictization and alteration. Five of the best available grains were analyzed. The data are concordant but show some spread along the Concordia curve that is attributed to some Pb loss (Fig. 4b). The three oldest zircon analyses overlap defining a Concordia age of 312.9 ± 2.0 Ma (Fig. 4b). Based on these data, we conclude that

Table 1
U–Pb data of granitic rocks from Segura, central Portugal.

	Mineral characteristics[a]	Weight (μg)[b]	U (ppm)[b]	Th/U[c]	Pbc[d] (pg)	$^{206}Pb/^{204}Pb$[e]	$^{207}Pb/^{235}U$[f]	2σ (abs.)	$^{206}Pb/^{238}U$[f]	2σ (abs.)	Rho	$^{206}Pb/^{238}U$[f]	$^{207}Pb/^{235}U$[f]	$^{207}Pb/^{206}Pb$[f]	2σ (abs.)
Two-mica granite (sample GTM)															
1	Z p [23]	64	477	0.18	2.7	34,962	0.35897	0.00088	0.04945	0.000011	0.96	311.2	311.4	313.6	1.6
2	Z lp [27]	83	372	0.18	8.8	10,874	0.35832	0.00087	0.04936	0.00010	0.96	310.6	311.0	313.7	1.7
3	Z lp fr [23]	56	262	0.17	2.5	18,229	0.35858	0.00086	0.04938	0.00010	0.94	310.7	311.2	314.3	1.9
4	Mz [3]	1	596	16.37	2.8	710	0.37952	0.00326	0.05243	0.00013	0.51	329.4	326.7	307.3	17.3
5	Mz [9]	1	604	22.60	2.4	815	0.36094	0.00309	0.04993	0.00013	0.52	314.1	312.9	304.4	17.0
Muscovite granite (sample GM)															
6	Z lp brooken [1]	1	939	0.04	1.6	1822	0.36515	0.00393	0.05018	0.00051	0.88	315.7	316.0	319.0	11.6
7	Z piece [1]	1	296	0.10	1.4	695	0.35920	0.00401	0.04978	0.00018	0.45	313.2	311.6	300.1	22.7
8	Z lp-fr [1]	1	323	0.15	1.8	596	0.36016	0.00513	0.04935	0.00029	0.50	310.5	312.3	325.8	27.8
9	Z tip [1]	2	934	0.05	3.0	1447	0.35304	0.00205	0.04882	0.00020	0.72	307.3	307.0	305.0	9.2
10	Z lp-fr [1]	1	155	0.37	2.8	187	0.34704	0.01293	0.04835	0.00031	0.43	304.4	302.5	288.1	78.0

[a] Z – zircon; Mz – monazite; p – prismatic; lp – long prismatic; fr – fractured; [N] – number of grains in fraction.
[b,d] Weight and concentrations are known to better than 10%, except for those near and below the ca. 1 μg limit of resolution of the balance.
[c] Th/U model ratio inferred from $^{208}Pb/^{206}Pb$ ratio and age of sample.
[d] Pbc is total common Pb in sample (initial + blank).
[e] Raw data corrected for fractionation.
[f] Corrected for fractionation, spike, blank and initial common Pb; error calculated by propagating the main sources of uncertainty; initial common Pb corrected using Stacey and Kramers (1975) model Pb.

two-mica granite and muscovite granite are essentially contemporaneous (Fig. 4).

6. Whole rock geochemistry

The average chemical analyses of major elements and selected trace elements of granites, granitic aplite veins and aplite-pegmatite veins from Segura are presented in Table 2. The granites and the aplite veins have a A/CNK ratio = molecular $Al_2O_3/(CaO + Na_2O + K_2O)$ which ranges from 1.12 to 1.27 and the lepidolite-subtype aplite-pegmatite veins yielded A/CNK values ranging between 1.20 and 1.43. Thus, all these granitic rocks are peraluminous and classified as Sn-bearing granite, with the highest Sn values in lepidolite-subtype granitic aplite-pegmatite (Sn: 293–327 ppm) (Table 2; Fig. 5). The normative corundum content ranges between 2.39 and 4.19%. The aplite-pegmatite veins have higher SiO_2, P_2O_5, F, Ta, Sn, Li, Y, Rb contents and lower TiO_2, total FeO, MgO and K_2O contents than the other granitic rocks from Segura (Fig. 5; Table 2). In the variation diagrams, two fractionation trends are indicated: (a) one for two-mica granite and lepidolite-subtype aplite-pegmatite veins, but with a gap in most trends; (b) another for muscovite granite and granitic aplite veins (Fig. 5). Rare earth element contents of selected samples of granitic rocks from Segura are given in Table 3 and the chondrite normalized rare-earth-element patterns from the granites are presented in Fig. 6. The two-mica granite has the highest ΣREE (131–172 ppm), is enriched in LREE relative to HREE (La_N/Lu_N) = 9–13 and has a negative Eu anomaly (Eu/Eu* = 0.28–0.30) (Fig. 6), whereas the muscovite granite (ΣREE = 21–27 ppm) and the aplite veins (ΣREE = 12–37 ppm) have irregular patterns (Table 3). The lepidolite-subtype aplite-pegmatite veins have a very low REE content (ΣREE < 12 ppm; Table 3). The suggestion, from variation diagrams with major and trace elements, that the two-mica granite and muscovite granite are not related (Fig. 5), is supported by their REE patterns, which are not subparallel (Fig. 6), and by the much higher Sr content of the muscovite granite (Table 2).

7. Isotopic data

Selected samples from granites, granitic aplite veins and lepidolite-subtype granitic aplite-pegmatite veins from Segura were analyzed for Rb–Sr and oxygen isotopes, which are listed in Table 4. The mean $(^{87}Sr/^{86}Sr)_{311}$ ratio and $\delta^{18}O$ of two-mica granite (0.7212 ± 0.0004; 12.8 ± 0.02‰) and muscovite granite (0.7163 ± 0.0009; 13.6 ± 0.12‰) support the inference that these granites cannot be mutually related and correspond to two distinct pulses of granite magma (Table 4), although both are derived by partial melting of metasedimentary materials. $(^{87}Sr/^{86}Sr)_i$ and $\delta^{18}O$ values are close in muscovite granite and granitic aplite veins confirming that these rocks are related to each other (Table 4). On the other hand, the decrease of $(^{87}Sr/^{86}Sr)_{311}$ and increase of $\delta^{18}O$, up to 1.6‰, from the two-mica granite to the aplite-pegmatite veins indicate isotopic disequilibrium and suggest that the aplite-pegmatite veins are not derived from the two-mica granite magma. The much lower $(^{87}Sr/^{86}Sr)_{311}$ value of these veins indicate that they crystallized from a more juvenile magma.

8. Mineral chemistry

8.1. Feldspar

Microcline compositions are uniform among all the granitic rocks (Or_{88} to Or_{98}; Table 5). Plagioclase is albite (An_0 to An_5),

Table 2
Average chemical analyses in wt.% and trace elements in ppm of granitic rocks from Segura, central Portugal.

Samples	Two-mica granite		Muscovite granite		Aplite veins		Lepidolite-subtype aplite-pegmatite	
	$n=5$	σ	$n=4$	σ	$n=3$	σ	$n=3$	σ
SiO_2	73.95	0.26	72.18	0.24	73.16	0.17	74.81	0.29
TiO_2	0.19	0.01	1.30	0.18	0.11	–	–	–
Al_2O_3	14.41	0.30	14.93	0.19	15.52	0.11	13.83	0.58
Fe_2O_3	0.17	0.09	0.08	0.04	0.25	0.13	0.34	0.06
FeO	1.19	0.10	0.40	0.07	0.42	0.13	0.45	0.07
MnO	0.02	–	0.06	–	0.09	0.01	0.04	0.01
MgO	0.34	0.02	0.10	0.02	0.03	–	–	–
CaO	0.55	0.03	0.69	0.05	0.54	0.05	0.49	0.02
Na_2O	3.82	0.25	4.46	0.14	4.64	0.05	3.95	0.28
K_2O	4.59	0.05	3.79	0.16	3.47	0.08	2.90	0.13
P_2O_5	0.36	0.01	1.28	0.59	0.75	0.02	2.23	0.32
H_2O+	0.69	0.10	0.83	0.16	0.75	0.29	1.24	0.13
Total	100.28		100.10		99.73		100.28	
F	1081	66	2167	121	2651	456	3767	368
Ga	21	–	36	–	35	–	35	–
Cr	17	–	16	–	10	–	7	–
W	10	–	13	–	[a]	–	7	–
V	14	–	[a]	–	[a]	–	[a]	–
Nb	14	–	43	–	55	28	86	8
Ta	[a]	–	17	–	35	–	55	6
Sn	23	–	45	6	70	13	310	17
Zn	46	–	54	–	67	4	62	–
Li	223	10	181	16	239	120	1080	156
Zr	82	–	28	–	25	–	22	8
Y	8	–	11	–	11	–	40	14
Sr	380	19	435	24	302	15	302	19
Pb	21	–	[a]	–	6	–	15	–
Ba	149	15	62	–	40	7	40	10
Rb	257	–	791	44	966	54	1502	252
Cs	49	–	32	–	50	6	[a]	–
U	10	–	26	6	14	–	10	–
Ge	[a]	–	[a]	–	5	–	9	–

n – number of analyzed samples, σ – standard deviation, (–) not detected. Analyst: I.M.H.R. Antunes.
[a] Below the limit of sensitivity, which is 5 ppm.

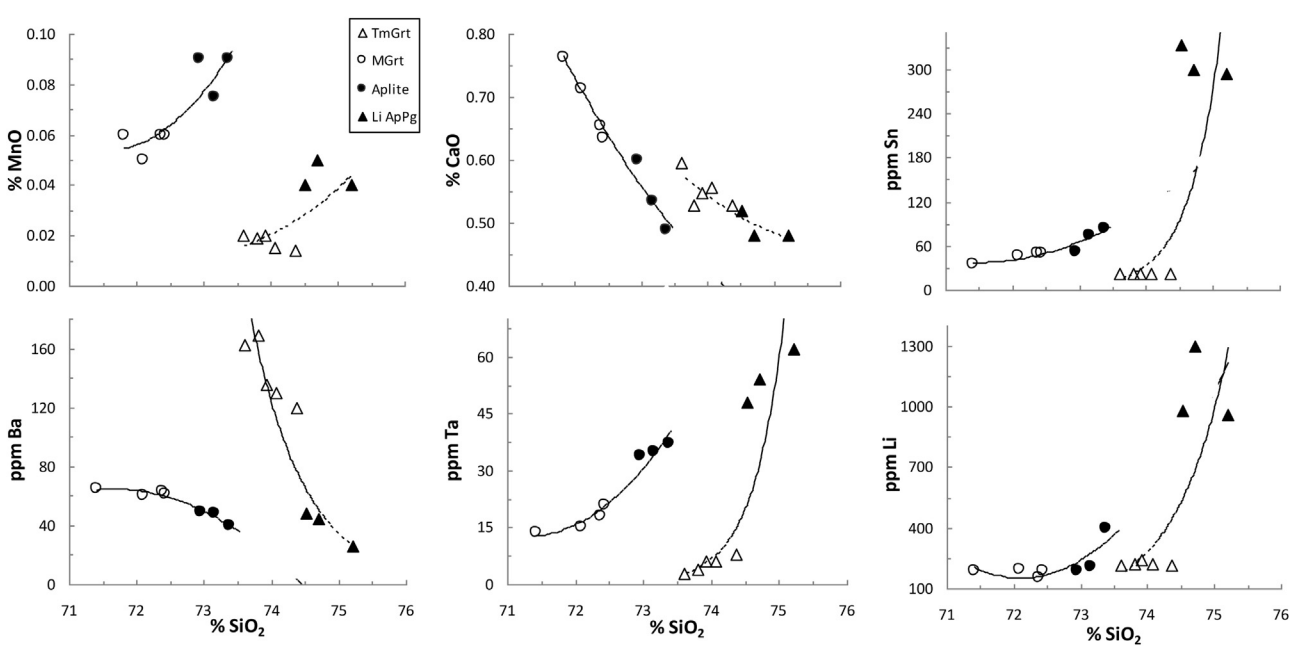

Fig. 5. Selected variation diagrams for major and trace elements vs. SiO_2. TmGrt – two-mica granite; MGrt – muscovite granite; aplite – granitic aplite veins; Li ApPg – lepidolite-subtype granitic aplite-pegmatite veins.

Table 3
Representative analyses of rare earth elements (ppm) of granitic rocks from Segura, central Portugal.

	Two-mica granite					Muscovite granite						Aplite veins					Lepidolite-subtype aplite-pegmatite veins			
	1	2	3	Average	σ	4	5	6	Average	σ	7	8	Average	σ	9	10	Average	σ
La	10.30	12.10	13.70	12.03	1.39	1.10	1.30	1.20	1.20	0.08	2.30	0.60	1.45	0.85	0.90	0.90	0.90	–
Ce	22.30	24.90	28.80	25.33	2.67	2.70	2.50	2.20	2.47	0.21	5.10	1.10	3.10	2.00	0.80	1.70	1.25	0.45
Pr	2.76	3.07	3.55	3.13	0.32	0.33	0.34	0.29	0.32	0.02	0.72	0.15	0.44	0.29	0.12	0.22	0.17	0.05
Nd	10.40	12.00	13.60	12.00	1.31	1.40	1.30	1.10	1.27	0.12	2.60	0.50	1.55	1.05	0.40	1.00	0.70	0.30
Sm	2.50	2.60	3.00	2.70	0.22	0.70	0.60	0.50	0.60	0.08	0.90	0.30	0.60	0.30	0.10	0.20	0.15	0.05
Eu	0.23	0.25	0.28	0.25	0.02	[a]	[a]	[a]	[a]	–	0.08	[a]	0.04	0.04	0.07	0.06	0.07	0.01
Gd	2.52	2.44	3.05	2.67	0.27	0.77	0.59	0.51	0.62	0.11	0.83	0.39	0.61	0.22	0.18	0.32	0.25	0.07
Tb	0.36	0.36	0.46	0.39	0.05	0.18	0.14	0.13	0.15	0.02	0.18	0.07	0.13	0.06	[a]	[a]	[a]	–
Dy	1.78	2.01	2.31	2.03	0.22	0.93	0.95	0.87	0.92	0.03	0.88	0.39	0.64	0.25	0.17	0.28	0.23	0.05
Ho	0.27	0.32	0.34	0.31	0.03	0.13	0.10	0.13	0.12	0.01	0.12	0.06	0.09	0.03	[a]	[a]	[a]	–
Er	0.69	0.82	0.86	0.79	0.07	0.31	0.23	0.29	0.28	0.03	0.26	0.15	0.21	0.06	0.13	0.13	0.13	–
Tm	0.08	0.11	0.15	0.11	0.03	0.06	[a]	[a]	0.02	0.03	[a]	[a]	[a]	–	[a]	[a]	[a]	–
Yb	0.60	0.90	0.90	0.80	0.14	0.40	0.30	0.30	0.33	0.05	0.30	0.20	0.25	0.05	0.10	0.10	0.10	0.00
Lu	0.08	0.11	0.15	0.11	0.03	[a]	0.05	[a]	0.02	0.02	[a]	[a]	[a]	–	[a]	[a]	[a]	–

σ – standard deviation. Analyses by the SGS Laboratory, Ontario, Canada.
[a] Below detection limit.

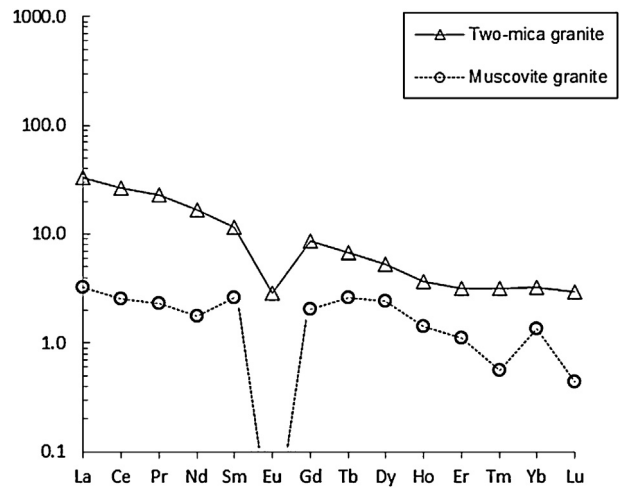

Fig. 6. Average chondrite-normalized REE abundances of two-mica granite and muscovite granite. Chondrite-normalized abundances were calculated using Taylor and McLennan (1985) values.

showing a slight decrease in Ca from two-mica granite to lepidolite-subtype aplite-pegmatite veins (Table 5).

Potassium feldspar has in general a higher average P_2O_5 content than coexisting plagioclase (e.g., London, 1992; Neiva, 1998; Breiter et al., 2005). Feldspars from muscovite granite and aplite veins have more P_2O_5 than feldspars from the other granitic rocks (Table 5). The P_2O_5 content of microcline is not related to its orthoclase content and the P_2O_5 content of albite does not depend on its anorthite content (Neiva, 1998). The empirical distribution coefficient D[P]Kf/Pl between K-feldspar and plagioclase is at 2.05 in the muscovite granite, 2.15 in the aplite veins and 1.36 in the aplite-pegmatite veins (Table 5), showing that no significant fractionation of phosphorous took place between coexisting feldspars from these rocks (London, 1992; Neiva, 1998), while equilibrium was only attained for the distribution of P between K-feldspar and plagioclase from the two-mica granite that yielded a D[P]Kf/Pl of 1.0.

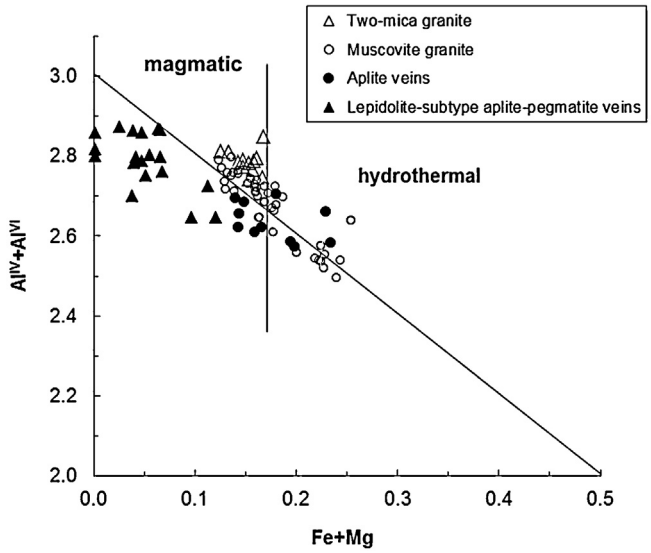

Fig. 7. Diagram of $Al^{IV} + Al^{VI}$ vs. Fe + Mg showing compositions of muscovites. The inclined line represents the theoretical substitution, while the vertical line separates the magmatic and hydrothermal field.

Table 4
Isotopic data of granitic rocks from Segura, central Portugal.

Granitic rocks	Rb (ppm)	Sr (ppm)	$^{87}Rb/^{86}Sr$	$^{87}Sr/^{86}Sr$	Error % (2σ)	$(^{87}Sr/^{86}Sr)_{311}$	$\delta^{18}O$
Two-mica granite							
GR2	280	340	0.8235	0.724550	0.001101	0.7207	12.82
GR4	240	400	0.5999	0.724311	0.001301	0.7216	12.84
H2	261	400	0.6521	0.724185	0.001522	0.7214	–
Muscovite granite							
M	862	415	2.0769	0.724310	0.000924	0.7151	13.42
M1S	781	434	1.7998	0.724308	0.000761	0.7163	–
M3	740	474	1.5614	0.724440	0.000846	0.7174	13.67
Aplite veins							
APL5	900	321	2.8037	0.724115	0.000710	0.7119	12.24
APL7	–	–	–	–	–	–	12.57
Lepidolite-subtype aplite-pegmatite veins							
PG1	–	–	–	–	–	–	14.49
PG2	–	–	–	–	–	–	14.32
PG3	1182	315	3.7524	0.724326	0.000634	0.7077	14.33

(–) Not determined. Sr isotopic analyses by the University of the Basque Country/EHU, Spain; Rb and Sr data by the University of Oviedo, Spain; $\delta^{18}O$ by the University of Western Ontario, Canada.

Table 5
Compositions of feldspars from granitic rocks of Segura, central Portugal.

Granitic rock	Two-mica granite	Muscovite granite	Aplite veins	Lepidolite-subtype aplite-pegmatite veins
Or content of K-feldspar	88–97	90–98	93–98	89–97
Wt.% BaO of K-feldspar	0.08	≤0.06	≤0.06	≤0.06
An content of plagioclase	0–5	0–1	0–3	0–1
Wt.% P_2O_5				
K-feldspar	0.46	1.31	1.42	0.57
Plagioclase	0.46	0.64	0.66	0.42
D[P]Kf/Pl (N)	1.00 (7)	2.05 (12)	2.15 (12)	1.36 (10)

D[P]Kf/Pl – empirical distribution coefficient. (*N*) – number of samples. Analyst: I.M.H.R. Antunes.

8.2. Muscovite

Representative compositions of analyzed muscovites from granitic rocks of Segura are given in Table 6. All granitic rocks contain mainly magmatic muscovite as suggested by their textural characteristics and chemistry (Fig. 7). Hydrothermal muscovite from muscovite granite and aplite veins has more Fe + Mg, but similar or less $Al^{IV} + Al^{VI}$ than magmatic muscovite (Fig. 7). Magmatic muscovites from two-mica granite and lepidolite-subtype aplite-pegmatite veins suggest fractionation trends, but a gap appears in each trend (Fig. 8). There is an increase in Si and Al^{VI} and decrease in Ti, Fe, Mg, Mg/(Mg + Fe) from primary muscovite of two-mica granite to muscovite of lepidolite-subtype aplite-pegmatite veins (Table 6; Fig. 8). Magmatic muscovites from muscovite granite and aplite veins have similar compositions and do not define fractionation trends (Fig. 8).

8.3. Lepidolite

Primary lepidolite is the main Li-bearing mineral from the lepidolite-subtype aplite-pegmatite veins (Table 6; Fig. 9a). It is younger and has more Si, F, Rb, Li, Cs, higher Rb/K and less $Al^{IV} + Al^{VI}$ than primary muscovite (Fig. 9b–d; Table 6). Microstructural evidence indicates that lepidolite replaces muscovite

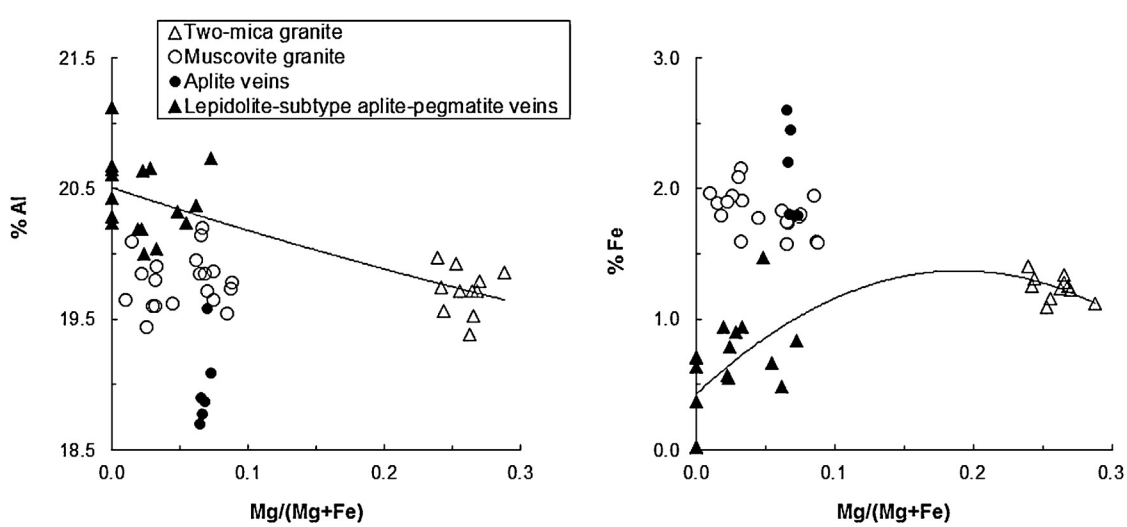

Fig. 8. Selected variation diagrams % Al vs. Mg/(Mg + Fe) and % Fe vs. Mg(Mg + Fe) for primary muscovites.

Table 6
Representative compositions of muscovite from granitic rocks of Segura, central Portugal.

	Muscovite				Lepidolite
	Two-mica granite	Muscovite granite	Aplite veins	Lepidolite-subtype aplite-pegmatite veins	Lepidolite-subtype aplite-pegmatite veins
SiO_2	45.52	46.41	46.38	47.08	53.49
TiO_2	0.15	0.12	0.27	0.02	0.03
Al_2O_3	35.32	34.11	33.08	36.34	25.21
FeO	1.51	2.88	3.24	0.81	0.12
MnO	0.04	0.05	0.07	0.13	0.45
MgO	0.68	0.17	0.28	0.04	0.02
CaO	–	0.02	–	0.01	0.02
BaO	0.03	0.03	0.01	0.02	0.03
Li_2O^*	0.16	0.85	0.69	0.38	4.48
Na_2O	0.75	0.64	0.53	0.52	0.30
K_2O	10.66	9.77	10.11	9.61	9.98
Rb_2O	0.02	–	–	0.03	0.84
Cs_2O	0.02	–	0.02	–	0.15
F	0.50	1.78	1.53	0.98	7.78
H_2O^*	4.23	3.64	3.72	4.08	0.89
	99.59	100.47	99.93	100.05	103.79
O≡F	0.21	0.75	0.64	0.41	3.27
Total	99.38	99.72	99.29	99.64	100.52
Si	3.055	3.102	3.126	3.106	3.500
Al^{IV}	0.954	0.898	0.874	0.894	0.500
ΣT	4.00	4.00	4.00	4.00	4.00
Al^{VI}	1.849	1.790	1.754	1.932	1.444
Ti	0.008	0.006	0.014	0.001	0.001
Fe^{2+}	0.085	0.161	0.183	0.045	0.007
Mn	0.002	0.003	0.004	0.007	0.025
Mg	0.068	0.017	0.028	0.004	0.002
Li^*	0.042	0.227	0.187	0.102	1.179
ΣR	2.05	2.20	2.17	2.09	2.66
Ca	–	0.001	–	0.001	0.001
Ba	0.001	0.001	–	0.001	0.001
Na	0.098	0.083	0.069	0.067	0.038
K	0.913	0.833	0.869	0.809	0.833
Rb	0.001	–	–	0.001	0.035
Cs	0.001	–	0.001	–	0.004
ΣA	1.01	0.92	0.94	0.88	0.91
F	0.106	0.376	0.326	0.204	1.610
OH^*	1.894	1.624	1.674	1.796	0.390

Compositions in wt.%. (–) Not detected. Calculated number of ions on the basis 12 oxygen atoms + F. Li_2O^* of muscovite values calculated from equation of Tischendorf et al. (1997); H_2O^* calculated by stoichiometry; OH^* calculated by difference to 2.000. Analyst: I.M.H.R. Antunes.

(Fig. 2b). Therefore it can be assumed that, initially, both micas did not grow side by side. The high Li, Rb, Cs and F contents of lepidolite suggest magmatic fractionation of the hydrous pegmatite melt (Černý et al., 1985; Charoy and Noronha, 1995).

8.4. Topaz

Topaz from lepidolite-subtype granitic aplite-pegmatite veins has a homogeneous composition, $Al_{2.0}(Si_{1.0}O_4)(F_{1.4}OH_{0.7})_{\Sigma 2.1}$ (Table 7), and a lower F content (13.59 wt.%) than the theoretical maximum value of F = 20.7 wt.% (Chang et al., 1997).

8.5. Tourmaline

The formula of tourmaline can be written as: $XY_3\,Z_6\,T_6O_{18}\,[BO_3]_3\,V_3\,W$, where X = Ca, Na, K, □ (vacancy); Y = Li, Mg, Fe^{2+}, Mn^{2+}, Al, Cr^{3+}, V^{3+}, Fe^{3+}; Z = Mg, Al, Fe^{3+}, V^{3+}, Cr^{3+}; T = Si, Al, B; B = B, (□); V = OH, O, (F) and W = OH, F, O (Hawthorne and Henry, 1999). The compositions of magmatic tourmalines from the two-mica granite and the aplite veins plot in the alkali group (Table 7; Fig. 10a and b) and are schorl (Fig. 10c). The main substitution schemes in these schorls are $(\square Al)(NaR)_{-1}$, deprotonation and $FeAl_{-1}$ (Fig. 10d and e). The schorl compositions from the two-mica granite and the aplite veins are distinct (Fig. 11), as expected.

8.6. Apatite

Apatite is the most abundant phosphate mineral in the Segura granitic rocks. Hydroxylapatite occurs in both granites and lepidolite-subtype aplite-pegmatite veins, but two-mica granite and muscovite granite contain fluorapatite as well, with less Ca than coexisting hydroxylapatite (Table 8). Calcium, Mn and F contents of apatite can be used as differentiation index (Chu et al., 2009; Neiva et al., 2011). Hydroxylapatite has more Ca in muscovite granite than in two-mica granite (Table 8), suggesting that these rocks are not related. However, fluorapatite in muscovite granite has less Ca and more Mn (and F) than in two-mica granite (Table 8). Hydroxylapatite from the aplite-pegmatite veins has a higher Ca and lower Mn contents than hydroxylapatite from the two-mica granite, suggesting that these veins are not related to the two-mica granite. Furthermore, fluorapatite that occurs in the two-mica granite was not recorded in the aplite-pegmatite veins. Phosphorous is a highly incompatible element and pegmatite crystallization promotes the gradual saturation of P and Li in the magma resulting in

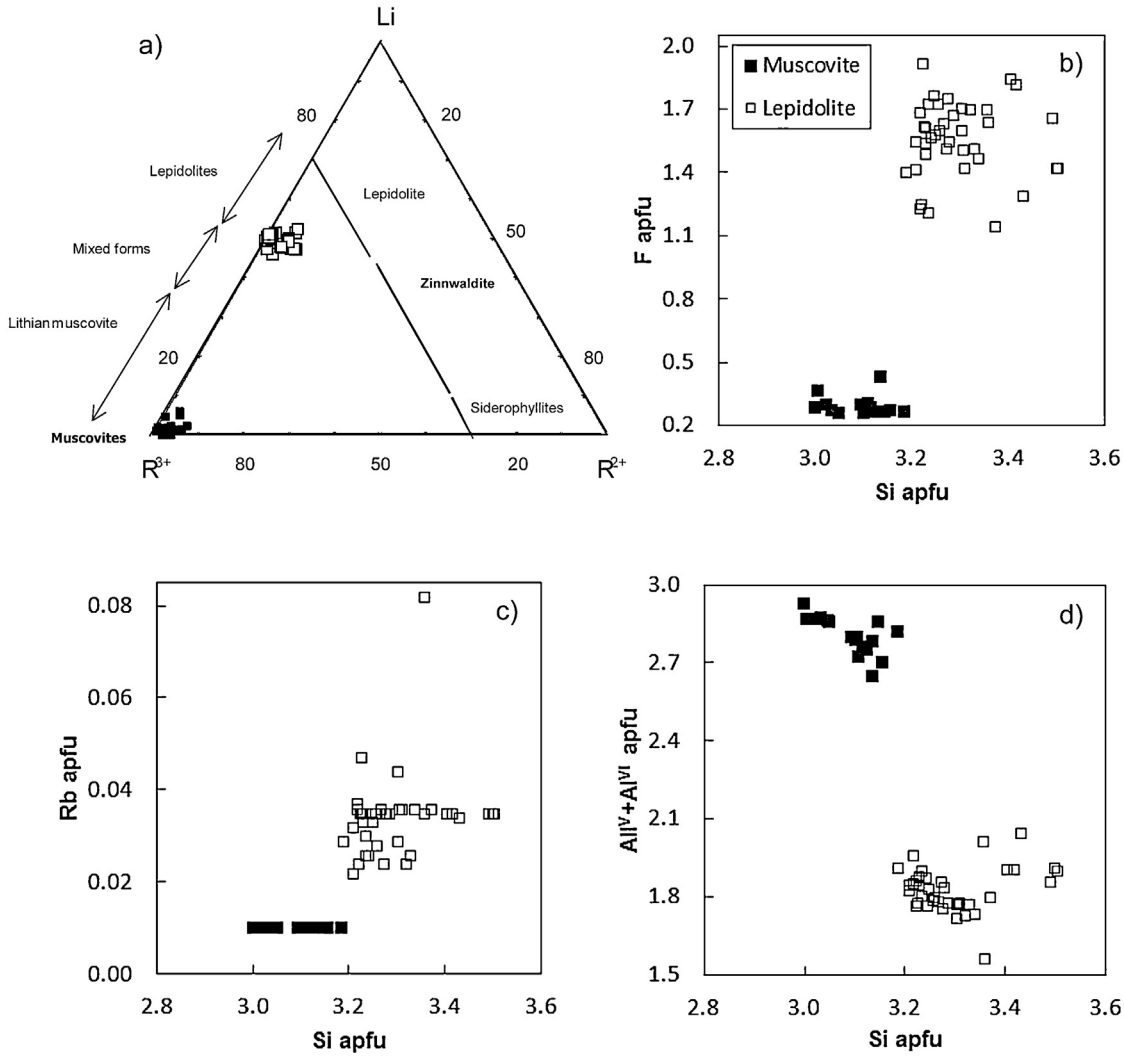

Fig. 9. (a) Plot of lepidolites from lepidolite-subtype aplite-pegmatite veins on the diagram Li-R^{3+}(Al^{VI} + Ti^{4+})–R^{2+}(Fe^{2+} + Mn + Mg), according to the classification of Foster (1960) modified by Rieder et al. (1999); (b–d) muscovite and lepidolite compositions in lepidolite-subtype aplite-pegmatite veins in the variation diagrams (apfu) F vs. Si, Rb vs. Si and Al^{IV} + Al^{VI} vs. Si.

crystallization of phosphate minerals, such as apatite and montebrasite (Hu et al., 2007).

8.7. Montebrasite

Amblygonite–montebrasite minerals can be the most representative phosphate mineral in some pegmatites (e.g., Hu et al., 2007; Pirard et al., 2007); especially of F- and Li-rich granitic pegmatites (Groat et al., 2003). The amblygonite–montebrasite solid-solution series has two end members: amblygonite LiAl[(PO_4)F] and montebrasite LiAl[(PO_4)(OH)] (e.g., Gaines et al., 1997). Primary montebrasite was found in lepidolite-subtype aplite-pegmatite veins from Segura (Table 8) and shows some deficiency in Al attributed to slight alteration (Neiva et al., 2000). Sodium and F mapping (Fig. 12), corroborated by electron microprobe analyses (Table 8), demonstrate that Na is heterogeneously distributed in the analyzed montebrasite crystals, but is concentrated in secondary lacroixite, similar to the Montebras pegmatite, Massif Central, France (Pirard et al., 2007) and the Eight Mile Park pegmatite, Colorado (Fransolet et al., 2007).

8.8. Cassiterite

In general, the analyzed cassiterite has Nb > Ta and Mn > Fe (Table 9), which is unusual (Neiva, 1996; Černý et al., 2004). In oscillatory zoned crystals, the darker zones have higher Nb and Ta contents than the lighter zones of the same crystal, the latter consisting of nearly pure SnO_2 (Table 9). Thus, in the darker zones pleochroism may be caused by Nb and Ta (Neiva, 1996). The unzoned crystals have a composition intermediate between that of light and dark zones (Table 9). Close to inclusions of tapiolite, ixiolite and microlite, which occur both in lighter and darker zones of the host, the cassiterite composition does not change. By contrast, cassiterite shows progressive compositional variations close to exsolved columbite that is only found in the darker zones where Ta and Nb increase, while Sn decreases with increasing distance from the exsolution products (Table 9). Furthermore, exsolved columbite occurs along fractures of cassiterite.

The analyses of cassiterite from lepidolite-subtype aplite-pegmatite veins are plotted in the (Sn,W,Ti)–(Nb,Ta)–(Fe,Mn) triangular diagram (Fig. 13a and b) and fall in the cassiterite field, close to the trend defined by the ideal substitution $(Fe,Mn)^{2+} + 2(Nb,Ta)^{5+} \leftrightarrows 3(Sn,Ti)^{4+}$ (Černý et al., 1985).

Table 7
Representative compositions of topaz from lepidolite-subtype aplite-pegmatite veins and tourmaline from two-mica granite and aplite veins of Segura, central Portugal.

	Topaz		Tourmaline	
	Lepidolite-subtype aplite-pegmatite		Two-mica granite	Aplite veins
SiO_2	32.62	SiO_2	35.30	35.05
Al_2O_3	56.29	TiO_2	0.35	0.38
FeO	0.01	B_2O_3 [a]	10.48	10.33
MgO	–	Al_2O_3	34.21	33.62
F	13.59	FeO	10.48	14.24
H_2O[a]	3.44	MnO	0.03	0.08
Total	105.95	MgO	3.35	0.63
O≡F	5.71	CaO	0.11	0.07
		Li_2O[a]	0.20	0.32
Total	100.24	Na_2O	1.88	1.90
		K_2O	0.03	0.04
Si	3.959	H_2O[a]	3.36	3.17
Al	0.041	F	0.54	0.84
Σ	4.00		100.32	100.67
Al	8.012	OH≡F	0.23	0.35
Fe	0.001			
Mg	–	Total	100.09	100.32
Σ	8.01			
F	5.540	Si	5.854	5.898
OH[a]	2.784	Al^{IV}	0.146	0.102
Σ	8.00	Al (Z)	6.000	6.000
		B	3.000	3.000
		Al (Y)	0.540	0.565
		Ti	0.044	0.048
		Fe^{2+}	1.453	2.004
		Mn	0.004	0.011
		Mg	0.828	0.158
		Li[a]	0.131	0.213
		Ca	0.020	0.013
		Na	0.604	0.620
		K	0.006	0.009
		□	0.370	0.359
		OH	3.717	3.553
		F	0.283	0.447

Compositions in wt.%. Calculated number of ions on the basis 24 oxygen atoms (topaz) and structural formula based on 31 anions (O, OH, F) in atoms per formula (tourmaline). (–) Not detected. Analyst: I.M.H.R. Antunes.
[a] Amount inferred from considerations of stoichiometry.

8.9. Nb–Ta-bearing oxide mineral

Chemical compositions of tapiolite-(Fe), ixiolite and microlite inclusions in cassiterite and exsolved columbite-(Fe), columbite-(Mn,Fe) and columbite-(Mn) from cassiterite of lepidolite-subtype aplite-pegmatite veins are given in Table 10. Tin, Ti, Sc and Mg are the most abundant minor elements in these inclusion and exsolution products. Chemical criteria (Neiva, 1996) were used to distinguish the relatively pure columbite-tantalite minerals from those of the ixiolite-wodginite series (Fig. 13c and d). Ixiolite inclusions have Nb > Ta, Fe > Mn and W > Ti (Table 10) and correspond to W-bearing ixiolite, which plots close to the $(Fe,Mn)(Nb,Ta)_2$–(Fe,Mn)(Sn,W,Ti) join (Fig. 13c). There is an evolution from exsolved columbite-(Fe) to columbite-(Mn) (Fig. 13e). Most Nb–Ta-bearing oxide minerals are finely zoned at the micrometre level making it impossible to determine the exact chemical composition of individual zones.

The chemical data suggest equilibrium between host cassiterite and columbite exsolutions.

Microlite inclusions are Ta-rich, with Ta/(Ta + Nb) values ranging from 0.69 to 0.90, F-rich, contains up to 4.6 wt.% F, and almost free of Ti (Table 10). Their compositions are similar to, but they contain more F than the primary microlite from the Varuträsk pegmatite, Sweden (Černý et al., 2004) and the Gonçalo aplite-pegmatite sills, Portugal (Neiva and Ramos, 2010).

9. Discussion and conclusions

9.1. Variscan granites and granitic aplite veins

The Variscan granitic rocks from Segura are peraluminous with a molecular ratio $Al_2O_3/(CaO + Na_2O + K_2O)$ of 1.12–1.27 and normative corundum values of ≥2.39%, a mean $(^{87}Sr/^{86}Sr)_i$ ranging from 0.7119 to 0.7212 and $\delta^{18}O$ of 12.4–13.5‰ (Tables 2 and 4). Consequently, these granites are of S-type character (Chappell and White, 1992, 2001). Judging from U–Pb dating of zircon and monazite, the two-mica granite crystallized at 311.0 ± 0.5 Ma and the muscovite granite at 312.9 ± 2.0 Ma (Fig. 4); they were emplaced during the syn- to late-D3 times of the Variscan Orogeny (Dias et al., 1998).

Two-mica granite and muscovite granite are not genetically related to each other, as suggested by major and trace elements of whole rocks and of muscovites (Figs. 5 and 8), their Sr contents (Table 2), whole rock REE patterns (Fig. 6), and distinct $(^{87}Sr/^{86}Sr)_i$ with mean values of 0.7212 and 0.7163, respectively (Table 4). Calcium and F contents of hydroxylapatite are distinct from those produced by fractional crystallization, because the Ca content increases from hydroxylapatite of two-mica granite to that of muscovite granite and the F content is similar in both (Table 8). Therefore, the two granites correspond to two distinct pulses of granite magma, probably derived by partial melting of heterogeneous metasedimentary materials. The whole rock CaO/Na_2O

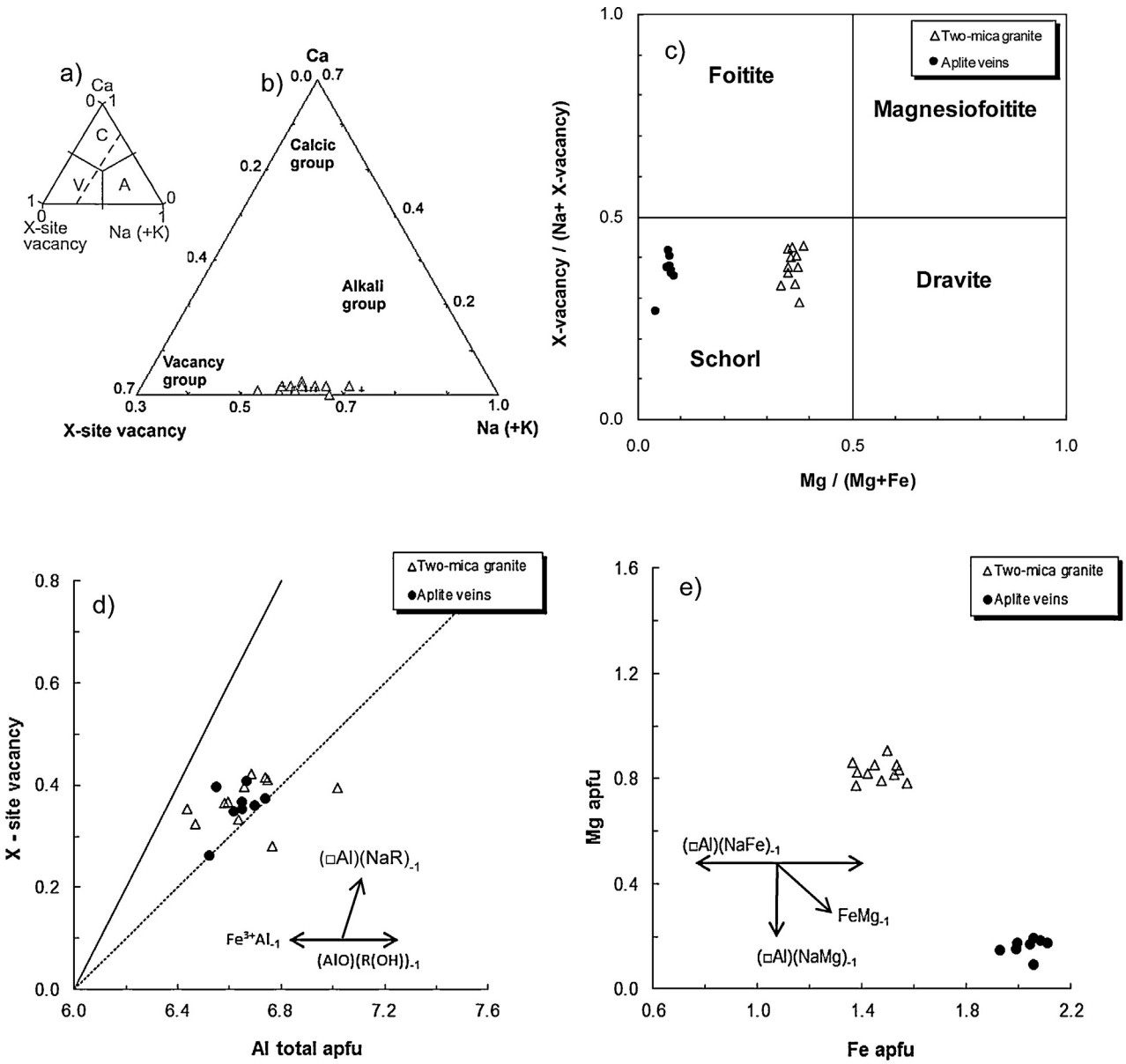

Fig. 10. Tourmaline compositions. (a) Classification of the principal tourmaline groups based on the X-site occupancy (from Hawthorne and Henry, 1999) showing the location of diagram (b), where all tourmaline plot in the Na (+K) group. (c) X-vacancy/(Na + X-vacancy) vs. Mg/(Mg + Fe) diagram. (d) X-site vacancy vs. total Al; R represents the sum of divalent cations, the solid line is parallel to the $(\square Al)(NaR)_{-1}$ vector, the dashed line is a reference line with a slope of 0.5. (e) Mg vs. Fe. Cations per formula unit were used.

values of 0.14 for the two-mica granite and 0.15 for the muscovite granite (Table 2), suggest that they are probably derived from partial melting of metapelitic rocks (Jung and Pfänder, 2007).

The aplite veins cannot be related to the two-mica granite, as shown by major and trace elements of granitic rocks and muscovite (Figs. 5 and 8) and distinct mean $(^{87}Sr/^{86}Sr)_{311}$ values of 0.7212 for the two-mica granite and 0.7119 for the aplite veins (Table 4). By contrast, major and trace elements suggest that the aplite veins are related to the muscovite granite by fractional crystallization (Fig. 5). This is supported by close mean $(^{87}Sr/^{86}Sr)_i$ values of 0.7119 and 0.7163 and $\delta^{18}O$ values of 12.4‰ and 13.5‰, respectively (Table 4), as well as by the increase of P_2O_5 in K-feldspar and albite from the muscovite granite to the aplite veins (Table 5).

Major elements were used to test whether the aplite veins can be derived from the muscovite granite magma by fractional crystallization, using a least-squares regression method. The sample of muscovite granite with the lowest SiO_2 content was used as the parent magma, and the composition of the other samples of muscovite granite and samples of aplite veins (without secondary muscovite and gormanite) where selected as residual melts. Pure quartz, anorthite, albite and K-feldspar and compositions of muscovite, apatite and ilmenite obtained by electron microprobe were used for the modeling. The sum of the squares of the residuals $((\Sigma R^2) \leq 0.830)$ shows that the test is acceptable since ΣR^2 must be <1 (Table 11). The anorthite content of plagioclase in the cumulate is similar to that of albite of muscovite granite, supporting the test.

Strontium, Ba and Rb are the most representative trace elements of granitic rocks and were also modeled. Their contents in the residual melt were calculated with two equations, one for perfect (or Rayleigh) fractional crystallization and another for equilibrium crystallization. We used the concentrations of Sr, Ba and Rb in the muscovite granite sample with the lowest SiO_2 content, the modal compositions of the cumulate and the weight fractions

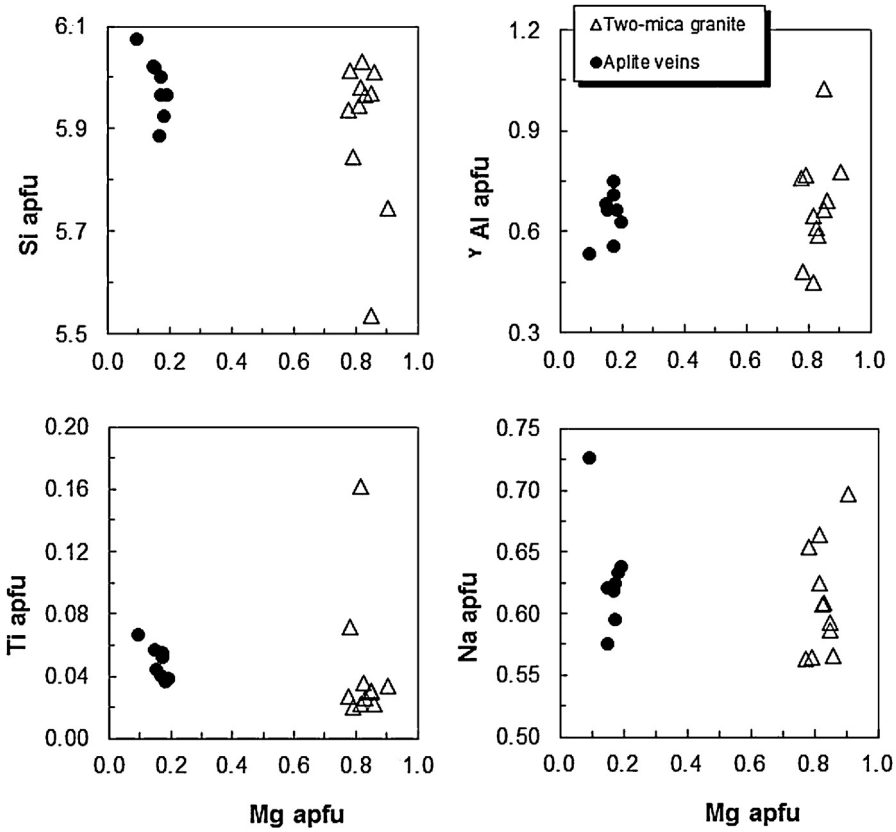

Fig. 11. Selected variation diagrams of schorl from two-mica granite and aplite veins at Segura, central Portugal.

Table 8
Representative compositions of phosphates from granitic rocks of Segura, central Portugal.

	Apatite						Montebrasite		Lacroixite	
	Two-mica granite		Muscovite granite		Lepidolite-subtype aplite-pegmatite veins		Lepidolite subtype aplite-pegmatite veins			
	a	b	a	b	a					
FeO	0.97	0.89	0.76	1.13	0.12	P_2O_5	49.87	49.73	44.93	45.35
MnO	1.37	1.28	1.51	3.53	0.57	Al_2O_3	34.22	33.60	31.59	32.02
MgO	–	0.01	0.02	0.01	0.01	FeO	–	–	0.02	0.03
CaO	52.75	52.29	53.78	49.72	54.89	MnO	–	–	–	–
Na_2O	0.13	0.14	0.18	0.08	0.27	MgO	–	–	0.03	0.01
K_2O	0.06	0.02	0.02	0.02	–	CaO	–	–	0.02	0.05
P_2O_5	42.93	42.80	41.75	42.20	41.84	Na_2O	0.25	1.03	15.02	13.06
F	0.01	5.13	0.01	5.39	0.01	Li_2O^*	10.38	9.97	2.21	3.24
Cl	0.01	0.01	–	–	–	F	2.03	1.05	10.44	10.03
H_2O^*	1.79	–	1.77	–	1.77	H_2O^*	4.52	4.69	0.42	0.72
	98.23	102.57	99.80	102.08	99.48		101.27	100.07	104.68	104.51
O≡F	–	2.15	–	2.26	–	O≡F	0.85	0.44	4.38	4.21
O≡Cl	–	–	–	–	–					
						Total	100.42	99.63	100.30	100.30
Total	100.01	100.42	99.80	99.82	99.48					
						P	1.000	1.000	1.000	1.000
P	3.039	3.048	2.983	3.046	2.987					
						Al	0.955	0.941	0.979	0.983
Mg	–	0.001	0.003	0.001	0.001	Fe	–	–	–	0.001
Fe	0.068	0.063	0.054	0.081	0.008	Mn	–	–	–	–
Mn	0.097	0.091	0.108	0.255	0.041	Mg	–	–	0.001	–
Na	0.021	0.023	0.029	0.013	0.044	Ca	–	–	0.001	0.001
K	0.006	0.002	0.002	0.002	–	Na	0.012	0.047	0.766	0.660
Ca	4.725	4.713	4.863	4.541	4.960	Li*	0.989	0.953	0.234	0.339
Σ	4.92	4.89	5.06	4.89	5.054	F	0.152	0.079	0.868	0.826
F	0.003	1.365	0.003	1.453	0.003	OH*	0.714	0.743	0.072	0.126
Cl	0.001	0.001	–	–	–	F+OH	0.866	0.822	0.940	0.952
OH*	0.996	–	0.997	–	0.997					
Σ	1.00	1.37	1.00	1.45	1.000					

(a) Hydroxylapatite; (b) fluorapatite. (–) Not detected. Compositions in wt.%. Atomic contents for apatite and montebrasite and lacroixite on the basis of 13 anions and 1P, respectively. Li_2O^*, Li*, H_2O^* and OH* based on charge balance. Analyst: I.M.H.R. Antunes; P.B. Silva.

Table 9
Representative compositions of cassiterite from lepidolite-subtype aplite-pegmatite veins of Segura, central Portugal.

	Cassiterite					
	Unzoned	Zoned		Zoned		
		(a)	(b)	(c)	(d)	(e)
WO_3	0.31	–	0.34	–	–	0.18
Ta_2O_5	1.22	0.59	1.46	0.15	1.56	2.42
Nb_2O_5	1.23	0.45	2.54	0.52	3.92	5.38
SnO_2	97.16	98.76	95.17	99.28	94.20	92.10
TiO_2	0.05	–	0.04	–	–	–
FeO	0.11	–	0.03	–	0.11	–
MnO	0.10	0.11	0.28	–	0.50	0.45
Total	100.18	99.91	99.86	99.95	100.29	100.53
W	0.002	–	0.002	–	–	0.001
Ta	0.008	0.004	0.010	0.001	0.011	0.016
Nb	0.014	0.005	0.029	0.006	0.044	0.060
Sn	0.966	0.987	0.945	0.991	0.926	0.899
Ti	–	–	0.001	–	–	–
Fe	0.002	–	0.001	–	0.002	–
Mn	0.002	0.002	0.006	–	0.010	0.009
Total	0.994	0.998	0.994	0.998	0.993	0.985
Ta/(Ta + Nb)	0.36	0.44	0.26	0.14	0.20	0.21
Mn/(Mn + Fe)	0.50	1.00	0.86	–	0.83	1.00

(a) Lighter zone, (b) darker zone of the same crystal. (c–e) Progressively increasing distance (10 μm) from exsolved columbite-(Mn) in a darker zone of cassiterite. Oxides in wt.%. (–) Not detected. Cation formula based on 2 atoms of oxygen. Analyst: I.M.H.R. Antunes.

Table 10
Representative compositions of inclusions and exsolution products in cassiterite from lepidolite-subtype aplite-pegmatite veins of Segura, central Portugal.

	Inclusions in cassiterite			Exsolution products from cassiterite				Inclusions in cassiterite	
	Tapiolite-(Fe)	Ixiolite		Columbite-(Fe)	Columbite-(Mn,Fe)	Columbite-(Mn)		Microlite	
WO_3	–	7.84	9.79	1.99	1.59	0.34	WO_3	0.46	0.78
Ta_2O_5	75.18	40.87	42.42	26.60	36.62	48.16	Ta_2O_5	74.55	74.84
Nb_2O_5	6.69	31.15	26.71	49.07	43.59	32.59	Nb_2O_5	4.85	5.27
UO_2	–	0.06	0.01	–	nd	–	TiO_2	0.09	0.11
ZrO_2	0.06	0.05	0.05	–	nd	0.07	UO_2	1.20	1.36
SnO_2	1.71	1.38	2.04	2.23	0.27	0.91	CaO	9.86	9.90
TiO_2	0.54	0.56	0.49	0.28	0.63	0.39	MnO	0.17	0.21
Sc_2O_3	0.56	0.32	0.35	0.21	nd	0.36	FeO	0.14	0.21
Bi_2O_3	–	0.03	–	–	nd	–	SnO	0.66	0.60
FeO	14.39	12.47	12.82	13.20	8.82	3.69	BaO	0.14	–
MnO	0.40	5.53	5.27	5.55	8.85	13.48	PbO	0.05	0.19
MgO	0.32	0.24	0.21	0.26	nd	0.24	Na_2O	4.71	4.68
							F	4.57	4.37
Total	99.85	100.50	100.16	99.39	100.37	100.23			
							Total	101.45	102.52
W	–	0.187	0.239	0.033	0.027	0.006			
Ta	1.647	1.022	1.086	0.463	0.654	0.908	O≡F	1.92	1.84
Nb	0.244	1.295	1.136	1.421	1.293	1.021			
U	–	0.001	–	–	nd	–	Total	99.53	100.68
Zr	0.002	0.002	–	–	nd	0.003			
Sn	0.055	0.051	0.077	0.057	0.007	0.025	U^{4+}	0.024	0.026
Ti	0.033	0.039	0.035	0.013	0.031	0.020	Ca^{2+}	0.933	0.921
Sc	0.039	0.026	0.029	0.012	nd	0.022	Ba^{2+}	0.005	–
Bi	–	0.001	–	–	nd	–	Mn^{2+}	0.013	0.015
Fe	0.969	0.959	1.009	0.707	0.484	0.214	Fe^{2+}	0.010	0.015
Mn	0.027	0.431	0.420	0.301	0.492	0.791	Sn^{2+}	0.026	0.023
Mg	0.038	0.033	0.030	0.024	nd	0.025	Pb^{2+}	0.001	0.004
							Na^{+}	0.806	0.787
Total	3.054	4.047	4.061	3.031	2.988	3.035	ΣA	1.818	1.791
							W^{6+}	0.010	0.018
Ta/(Ta + Nb)	0.87	0.44	0.49	0.25	0.34	0.47	Ta^{5+}	1.790	1.768
Mn/(Mn + Fe)	0.03	0.31	0.29	0.30	0.50	0.79	Nb^{5+}	0.194	0.207
							Ti^{4+}	0.006	0.007
							ΣB	2.00	2.000
							F^{-}	1.276	1.199
							$(OH)^{-}$	–	–
							O^{2-}	5.800	5.829
							Σ anions	7.076	7.028
							Ta/(Ta + Nb)	0.90	0.90

Oxides in wt.%. (–) Not detected; nd – not determined. Cation formula based on 6 atoms of oxygen for tapiolite-(Fe) and columbite and 8 atoms of oxygen for ixiolite. Microlite formula contents based on (Ta + Nb + Ti + W) = 2; $(OH)^{-}$ calculated as charge-balanced complement to Σ anions = 7. Microlite Sc_2O_3, Sb_2O_3, Bi_2O_3 and Cs_2O contents were not detected. Analyst: P.B. Silva; I.M.H.R. Antunes.

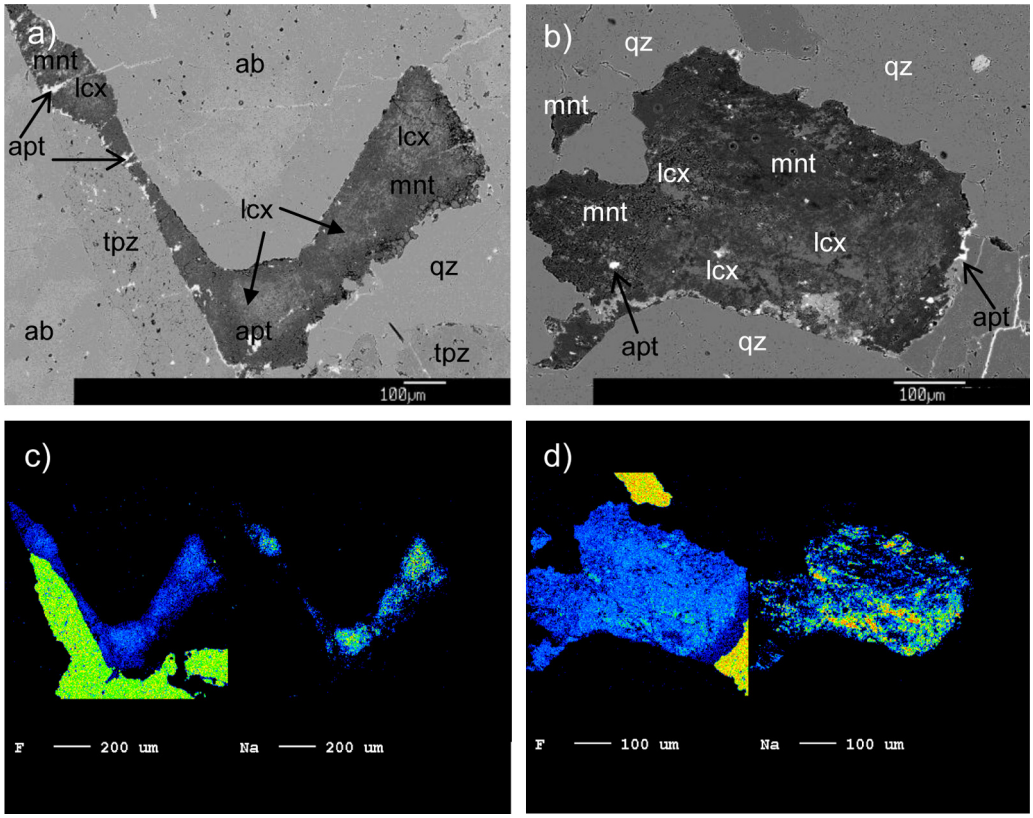

Fig. 12. Compositional variation in montebrasite from lepidolite-subtype aplite-pegmatite veins. (a and b) Crystal of montebrasite (mnt) showing lacroixite-rich areas (lcx). Montebrasite has apatite (apt) inclusions and is associated with topaz (tpz), quartz (qz) and albite (ab). (c and d) Sodium and F maps of lacroixite-rich areas of a montebrasite sample (a) and (b), respectively where montebrasite is dark gray and lacroixite is lighter gray.

Table 11
Results of the fractional crystallization modeling from muscovite granite to aplite veins of Segura, central Portugal.

	Determined parent granite	Calculated composition of parent magma for	
	M3	Muscovite granite M1S	Aplite veins Apl5
SiO_2	73.60	73.60	73.70
TiO_2	1.30	1.30	0.80
Al_2O_3	15.10	15.10	15.00
Fe_2O_3t	0.60	0.60	1.00
MgO	–	–	–
CaO	0.80	0.70	0.90
Na_2O	4.80	4.70	4.80
K_2O	3.80	3.70	3.80
FR		0.644 ± 0.037	0.439 ± 0.257
$\sum R^2$		0.002	0.830
Modal composition of cumulate			
Quartz		25.9 ± 2.8	27.3 ± 11.9
Plagioclase		49.6 ± 5.0	46.7 ± 24.4
K-feldspar		23.1 ± 2.5	23.2 ± 11.0
Ilmenite		1.4 ± 0.0	2.8 ± 0.7

Composition of residual melts

ppm	Det.	Det.	Calc.	Det.	Calc.
Sr	474	434	283	321	199
Ba	65	60	51	49	41
Rb	740	781	1101	900	1555

Fe_2O_3t – total Fe_2O_3; FR – weight fraction of melt remaining during fractional crystallization; ΣR^2 – sum of the squares of the residuals; (–) not detected. Det. – determined; Cal. – calculated. Distribution coefficients for Sr, Ba and Rb from Peccerillo et al. (1994).

of the remaining melt during fractional crystallization and the distribution coefficients of Peccerillo et al. (1994). The values calculated using the Rayleigh fractionation equation are the closest to the analytical data. Strontium and Ba decrease and Rb increases with the decrease in the weight fraction of the remaining melt during fractional crystallization from the muscovite granite to the aplite veins (Table 11). Modeling only shows general trends due to the large uncertainties of the weight fractions of the melt remaining during fractional crystallization and of the distribution coefficients. The aplite veins are derived from the muscovite granite magma by fractional crystallization of quartz, plagioclase, K-feldspar and ilmenite (Table 11).

9.2. Lepidolite-subtype aplite-pegmatite veins

Variation diagrams for major and trace elements of granitic rocks and muscovite suggest fractionation trends from two-mica granite to lepidolite-subtype aplite-pegmatite veins, but with a gap (Figs. 5 and 8). The fractional crystallization is supported by the increasing P_2O_5 content of microcline and decreasing anorthite content of plagioclase from the two-mica granite to the aplite-pegmatite veins (Table 5). However, the hydroxylapatite compositions (Table 8) do not support this mechanism, because the behaviors of Ca, Mn and F are opposite to the expected. In fact, Ca increases, Mn decreases and F remains constant from the hydroxylapatite of the two-mica granite to that of the aplite-pegmatite veins. Furthermore, the mean $(^{87}Sr/^{86}Sr)_{311}$ and $\delta^{18}O$ values (Table 4) are distinct for the two-mica granite (0.7212; 12.8‰) and the aplite-pegmatite veins (0.7077; 14.4‰), indicating that these rocks are not related to each other. The lepidolite-subtype aplite-pegmatite veins are also not related to the sequence defined by muscovite granite and aplite veins, as shown by the

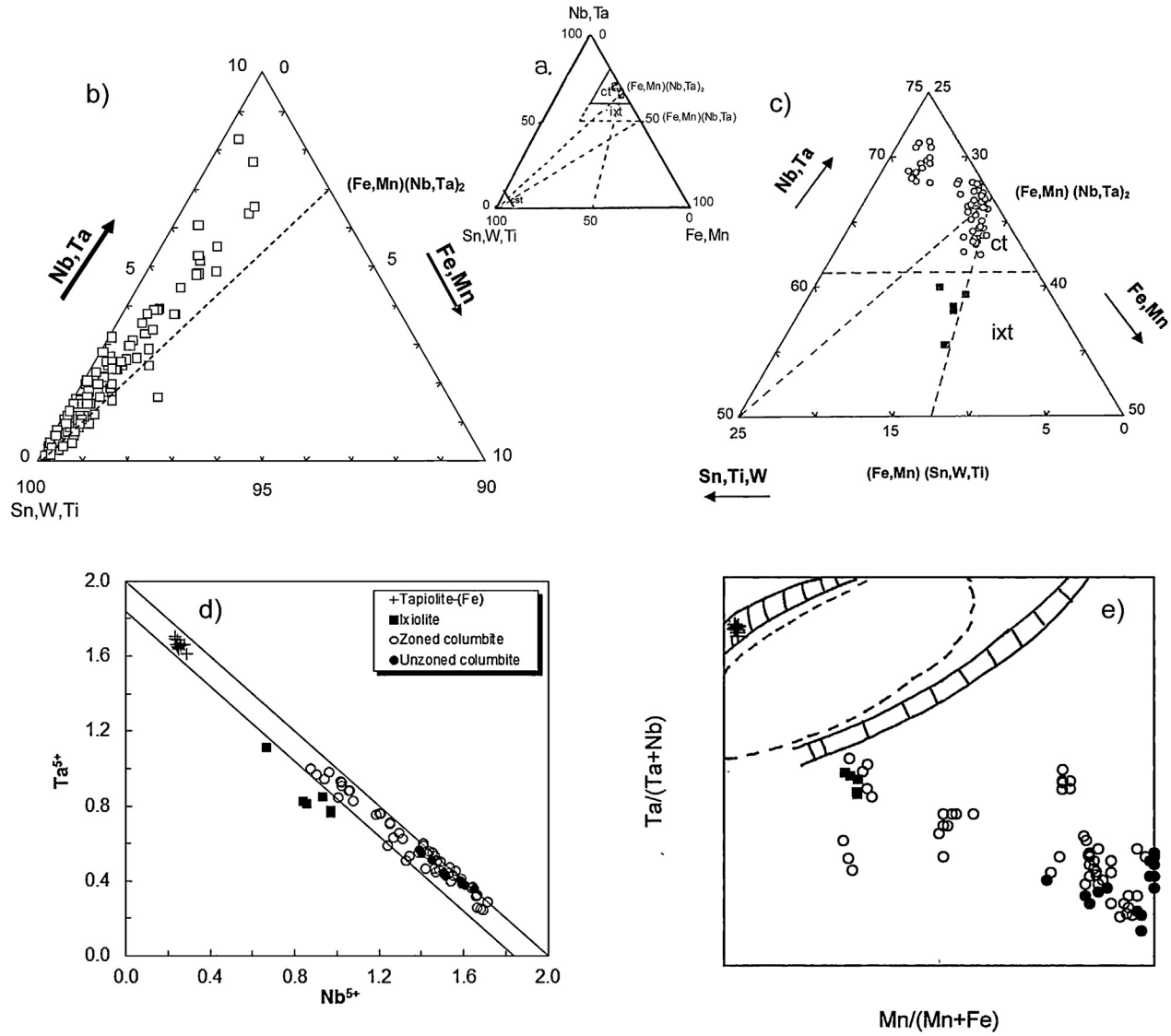

Fig. 13. Compositions of cassiterite, columbite group and ixiolite minerals from lepidolite-subtype aplite-pegmatite veins, plotted on the: (a–c) (Sn,W,Ti)–(Nb,Ta)–(Fe,Mn) diagram showing cassiterite (cst), columbite (ct) and ixiolite (ixt) fields; (d) plot of Nb^{5+} vs. Ta^{5+} (Neiva, 1996); (e) quadrilateral compositional diagram Ta/(Ta + Nb) vs. Mn/(Mn + Nb) (Černý, 1992).

variation diagrams for major and trace elements of granitic rocks and muscovite (Figs. 5 and 8). The aplite-pegmatite veins display the lowest $(^{87}Sr/^{86}Sr)_{311}$ ratio of 0.7077 and the highest $\delta^{18}O$ value of 14.4‰ (Table 4); they have lower P_2O_5 contents of K-feldspar and plagioclase than in those of muscovite granite and aplite veins (Table 5), and less Mn, more Ca and similar F in hydroxylapatite than in that from the muscovite granite (Table 8). Although, lepidolite-subtype aplite-pegmatite veins and granites from Segura are separated by less than 2 km, i.e. within the defined distance from potential granite parents (Černý et al., 2005), these veins may be derived from a younger granite magma, probably far away, as lepidolite-subtype pegmatite melts may migrate over long distances (Černý et al., 2005). Other Portuguese lepidolite-subtype aplite-pegmatite sills from Gonçalo are derived from a biotite > muscovite granite magma by fractional crystallization of quartz, plagioclase, K-feldspar, biotite and ilmenite, but magmatic fluids controlled their Rb and Ba contents (Neiva and Ramos, 2010).

Trace elements Rb, Li and Sn, which increase with fractional crystallization, of lepidolite-subtype aplite-pegmatite veins from Segura were compared with those of similar aplite-pegmatites from the Iberian Massif in Portugal and Spain. The Segura aplite-pegmatite veins are less evolved than those from Gonçalo, Barroso-Alvão and Fregeneda-Almendra, because they have lower Rb, Li and Sn average contents (Table 12). But they are more evolved than aplite-pegmatites of Arga, as they have higher Rb, Li and Sn average contents than them (Table 12).

Lepidolite-subtype aplite-pegmatite veins from Segura contain muscovite, lepidolite, topaz, hydroxylapatite, montebrasite and microlite (Tables 6, 7, 8 and 10), which suggest that these veins are enriched in Li, F and P as found in other pegmatites (e.g., Pal et al., 2007; Neiva and Ramos, 2010). These elements lower the solidus temperature and viscosity of the magma (London, 1992). Consequently, pegmatites enriched in these elements are often more fractionated than those depleted in these elements, as the solidus temperature can decrease below 500 °C (London, 1992). Tourmaline was not found in lepidolite-subtype aplite-pegmatite veins from Segura, because the pegmatite melt did not contain sufficient iron to form schorl and lithium to form elbaite, as lithium is mainly retained in lepidolite. Boron migrated to the country rock, where metasomatic tourmaline crystallized. The Portuguese lepidolite-subtype aplite-pegmatites from Vieiros and Gonçalo contain magmatic tourmaline, but metasomatic tourmaline occurs

Table 12
Average trace element contents of Portuguese and Spanish lepidolite-subtype granitic aplite-pegmatites.

	Segura		Gonçalo		Barroso-Alvão	Arga		Fregeneda-Almendra	
	Central Portugal				Northern Portugal			Spain-Portugal	
	Average	σ	Average	σ	Average	Average	σ	Average	σ
Determined									
ppm									
Rb	1502	252	1834	446	2393	415	207	4870	2603
Li	1080	156	5291	2360	3565	378	213	4921[a]	1005
Sn	310	17	532	348	728	218	307	n.d.	307
n	3		8		1	10		3	
References	This study		Neiva and Ramos (2010)		Lima (2000) Martins (2009)	Leal Gomes (1994)		Vieira (2010)	

n – number of analyses; σ – standard deviation; n.d. – not determined.
[a] Calculated.

in the adjacent host rocks (Neiva et al., 2007; Neiva and Ramos, 2010).

Rare occurrences of cassiterite with Mn > Fe (Table 9) are restricted to the lepidolite-enriched granitic pegmatites (Černý et al., 2004), but the same also occurs in cassiterite from amblygonite-subtype aplite-pegmatite sills from Gonçalo (Neiva and Ramos, 2010). Exsolutions of columbite-(Fe) evolved to columbite-(Mn) (Table 10; Fig. 13). The increase in Mn/(Mn + Fe) ratio of columbite also occurs in lepidolite-subtype aplite-pegmatite sills from Gonçalo, where tantalite-(Mn) also appears.

In aplite-pegmatite veins from Segura, F is retained in muscovite, lepidolite, topaz, montebrasite and microlite. Melt evolution resulted in increased fluorine activity, as shown by the microlite composition. In situ magma fractionation is associated with rare-element-enriched and Li-bearing minerals as found in granitic pegmatites from Separation Lake area, Ontario, Canada (Tindle and Breaks, 2000) and Gonçalo, central Portugal (Neiva and Ramos, 2010). The presence of microlite and topaz in aplite-pegmatite veins from Segura are indicators of advanced fractionation and the compositions of these minerals reflect the volatiles in the pegmatite melt (Tindle and Breaks, 2000). Primary microlite is very Ta-rich and contains more Ta than coexisting columbite (Table 10) as was found in other areas (e.g., Černý et al., 2004; Wise and Černý, 1990; Neiva and Ramos, 2010). Microlite accompanied by columbite-(Mn) is found in the more evolved F-rich varieties of rare-element pegmatites from Separation Lake, Ontario, Canada (Tindle and Breaks, 2000) and Gonçalo, northern Portugal (Neiva and Ramos, 2010).

Acknowledgements

Thanks are due to Prof. Machado Leite (S. Mamede de Infesta, Portugal) for electron microprobe facilities; Prof. R. Nesbitt and Prof. I.W. Croudace (Southampton, UK) for the XRF facilities; Prof. B.J. Wood (University of Bristol, UK) for the EUGF-Bristol research facility given to I.M.H.R. Antunes to use the electron microprobe; Prof. Gil Ibarguchy (University of the Basque Country, Spain) for the isotopic Sr determinations, Prof. A. Cuesta (University of Oviedo, Spain) for the Rb and Sr whole rock contents and Prof. F.J. Longstaffe (University of Western Ontario, Canada) for the oxygen isotope analyses. Financial support was provided from the Portuguese Government for the project Pest-OE/CTE/UI0073/2011 of Geosciences Centre through the Portuguese Foundation for Science and Technology. This paper benefited from the helpful comments of Prof. Stefan Jung and Prof. Martin Okrusch.

References

Antunes, I.M.H.R., Neiva, A.M.R., Silva, M.M.V.G., 2002. The mineralized veins and the impact of old mine workings on the environment at Segura, central Portugal. Chem. Geol. 190, 417–431.
Antunes, I.M.H.R., Neiva, A.M.R., Silva, M.M.V.G., Corfu, F., 2008. Geochemistry of S-type granitic rocks from the reversely zoned Castelo Branco pluton (central Portugal). Lithos 103, 445–465.
Antunes, I.M.H.R., Neiva, A.M.R., Silva, M.M.V.G., Ramos, J.M.F., Silva, P.B., 2009. Geochemistry of Li-bearing aplite-pegmatite veins from Cabeço Queimado and associated granitic rocks (Segura, central Portugal). In: Estudos Geologicos, 19/2, Contributions of the 4th International Symposium on Granitic Pegmatites – Pegm2009, Brazil, pp. 40–44.
Beurlen, H., Marcelo, R.R.S., Castro, C., 2001. Fluid inclusions in Be–Ta (Li–Sn)-bearing pegmatites from the Borborema Province, Northeast Brazil. Chem. Geol. 173, 107–123.
Breiter, K., Müller, A., Leichmann, J., Gabašová, 2005. Textural and chemical evolution of a fractionated granitic system: the Podlesí stock, Czech Republic. Lithos 80, 323–345.
Černý, P., 1992. Geochemical and petrogenetic features of mineralization in rare-element granitic pegmatites in the light of current research. Appl. Geochem. 7, 393–426.
Černý, P., Chapman, R., Ferreira, K., Smeds, S.A., 2004. Geochemistry of oxide minerals of Nb, Ta, Sn and Sb in the Varuträsk granitic pegmatite, Sweden: the case of an anomalous columbite-tantalite trend. Am. Mineral. 89, 505–518.
Černý, P., Ercit, 2005. The classification of granitic pegmatites revisited. Can. Mineral. 43, 2005–2026.
Černý, P., Massau, M., Goad, B.E., Ferreira, K., 2005. The Greer Lake leucogranite, Manitoba, and the origin of lepidolite-subtype granitic pegmatites. Lithos 80, 305–321.
Černý, P., Meintzer, R.E., Anderson, A.J., 1985. Extreme fractionation in rare-element granitic pegmatites: selected examples of data and mechanisms. Can. Mineral. 23, 381–421.
Chang, L.L.Y., Howie, R.A., Zussman, J., 1997. Rock Forming Minerals – Orthosilicates, vol. I-A., 2nd edition, pp. 801–815.
Chappell, B.W., White, A.J.R., 1992. I- and S-type granites in the Lachland Fold Belt. Trans. R. Soc. Edinb.: Earth Sci. 83, 1–26.
Chappell, B.W., White, A.J.R., 2001. Two contrasting granite types: 25 years later. Aust. J. Earth Sci. 48, 489–499.
Charoy, B., Noronha, F., 1995. A multistage model for growth of a rare element, volatile rich microgranite: the example of Argemela (Portugal). J. Petrol. 37, 73–94.
Chu, M.F., Wang, K.L., Griffin, W.L., Chung, S.L., O'Reilly, S.Y., Pearson, N.J., Iizuka, Y., 2009. Apatite composition: tracing petrogenetic processes in Transhimalayan granitoids. J. Petrol. 50, 1829–1855.
Corfu, F., 2004. U–Pb geochronology of the Leknes Group: an exotic Early Caledonian metasedimentary assemblage stranded on Lofoten basement, northern Norway. J. Geol. Soc., Lond. 161, 619–627.
Corfu, F., Evins, P.M., 2002. Late Paleoproterozoic monazite and titanite U–Pb ages in the Archean Suomujärvi complex, N Finland. Precambrian Res. 116, 171–181.
Cotelo Neiva, J.M., 2006. Structures of granitic aplites and pegmatites. In: Mirão, J., Balbino, A. (Eds.), Proceedings from VII National Geological Congress. Estremoz, Portugal, pp. 1149–1155 (in Portuguese).
Croudace, I.W., Thorpe, O.W., 1988. A low dilution, wavelength dispersive X-ray fluorescence procedure for the analysis of archaeological rock artefacts. Archaeometry 30, 227–236.
Croudace, I.W., Gilligan, J., 1990. Versatile and accurate trace element determinations in iron-rich and other geological samples using X-ray fluorescence analysis. X-ray Spectrom. 19, 117–123.
Currie, K.L., Whalen, J.B., Davis, W.J., Longstaffe, F.J., Cousens, B.L., 1998. Geochemical evolution of peraluminous plutons in southern Nova Scotia, Canada – a pegmatite-poor suite. Lithos 44, 117–140.
Dias, G., Leterrier, J., Mendes, A., Simões, P.P., Bertrand, J.M., 1998. U–Pb zircon and monazite geochronology of post-collisional Hercynian granitoids from the Central Iberian Zone (Northern Portugal). Lithos 45, 349–369.
Fransolet, A.-M., Fontan, F., De Parseval, P., 2007. Natromontebrasite, a discredited mineral species. Can. Mineral. 45, 391–396.
Foster, M.D., 1960. Interpretation of the composition of lithium micas. U.S. Geol. Surv. Prof. Paper 354-B, 1–49.

Gaines, R.V., Skinner, H.C.W., Foord, E.E., Mason, B., Rosenzweig, A., 1997. Dana's New Mineralogy, 8th edition. John Willey & Sons, Inc.
Groat, L.A., Chakoumakos, B.C., Brouwer, D.H., Hoffman, M., Fyfe, C.A., Morell, H., Schultz, A.J., 2003. The amblygonite ($LiAlPO_4F$)–montebrasite ($LiAlPO_4OH$) solid solution: a combined powder and single-crystal neutron diffraction and solid-state Li MAS, CP MAS and REDOR NMR study. Am. Mineral. 88, 195–210.
Hawthorne, F.C., Henry, D.J., 1999. Classification of the minerals of the tourmaline group. Eur. J. Mineral. 11, 201–215.
Hu, H., Wang, R.C., Fontan, F., Zhang A., Chen, J., 2007. Phosphate minerals from the Nanping pegmatite, SE China. In: Martins, T., Vieira, R. (Eds.), Granitic Pegmatites: The State of the Art, Memórias n° 8, pp. 46–47.
Jaffey, A.H., Flynn, K.F., Glendenin, L.E., Benthey, W.C., Essling, A.M., 1971. Precision measurement of halflives and specific activities of ^{235}U and ^{238}U. Phys. Rev. C: Nucl. Phys. 4, 1889–1906.
Jung, S., Pfänder, J.A., 2007. Source composition and melting temperatures of orogenic granitoids: constrains from CaO/Na_2O, Al_2O_3/TiO_2 and accessory mineral saturation thermometry. Eur. J. Mineral. 19, 859–870.
Kalt, A., Corfu, F., Wijbrans, J.R., 2000. Time calibration of a P-T path from a Variscan high-temperature low-pressure metamorphic complex (Bayerische Wald, Germany) and the detection of inherited monazite. Contrib. Mineral. Petrol. 138, 143–163.
Krogh, T.E., 1982. Improved accuracy of U/Pb zircon ages by creation of more concordant systems using air abrasion technique. Geochim. Cosmochim. Acta 46, 637–649.
Leal Gomes, C., 1994. Estudo estrutural e paragenético de um sistema pegmatóide granítico – o campo aplito-pegmatítico de Arga, Minho – Portugal. Unpublished PhD Thesis. Minho University, Portugal, p. 695.
Leal Gomes, C., 2006. Paragenetic analysis of state transition and paroxysmal evolution in granitic pegmatite systems of Central-Iberian Pegmatite Belt – structural, mineralogical and geochemical data. In: Mirão, J., Balbino, A. (Eds.), Proceedings from VII National Geological Congress. Estremoz, Portugal, pp. 1169–1175 (in Portuguese).
Lima, A.M.C., 2000. Estrutura, mineralogia e génese dos filões aplitopegmatíticos com espodumena da região Barroso-Alvão. Unpublished PhD Thesis. Porto University, Portugal, p. 270.
Linnen, R.L., Cuney, M., 2005. Granite-related rare-element deposits and experimental constrains on Ta–Nb–W–Sn–Zr–Hf mineralization. In: Linnen, R.L., Sampson, I.M. (Eds.), Rare Element Geochemistry and Mineral Deposits, vol. 17. Geological Association of Canada Short Course Notes, St. Catharines, pp. 45–68.
London, D., 1992. The application of experimental petrology to the genesis and crystallization of granitic pegmatites. Can. Mineral. 30, 499–540.
Ludwig, K.R., 2003. Isoplot 3.0. A Geochronological Toolkit for Microsoft Excel. Berkeley Geochronology Center Special Publication No. 4, p. 70.
Martins, T.C., 2009. Multidisciplinary study of pegmatites and associated Li and Sn–Nb–Ta mineralization from the Barroso-Alvão region. Unpublished PhD Thesis. Porto University, Portugal, p. 192.
Mattinson, J.M., 2005. Zircon U–Pb chemical abrasion ("CA-TIMS") method: combined annealing and multi-step partial dissolution analysis for improved precision and accuracy of zircons ages. Chem. Geol. 220, 47–66.
Neiva, A.M.R., 1996. Geochemistry of cassiterite and its inclusions and exsolution products from tin and tungsten deposits in Portugal. Can. Mineral. 34, 745–768.
Neiva, A.M.R., 1998. Phosphorous in highly peraluminous granites between Douro and Tamega valleys, northern Portugal. Acta Univ. Carolin.: Geol. 42 (1), 80–82.
Neiva, A.M.R., Silva, M.M.V.G., Antunes, I.M.H.R., Ramos, J.M.F., 2000. Phosphate minerals of some granitic rocks and associated quartz veins from northern and central Portugal. J. Czech Geol. Soc. 45 (3–4), 35–43.
Neiva, A.M.R., Gomes, M.E.P., Ramos, J.M.F., Silva, P.B., 2008. Geochemistry of granitic aplite-pegmatite sills and their minerals from Arcozelo da Serra area (Gouveia, central Portugal). Eur. J. Mineral. 20, 465–485.
Neiva, A.M.R., Ramos, J.M.F., 2010. Geochemistry of granitic aplite-pegmatite sills and petrogenetic links with granites, Guarda-Belmonte area, central Portugal. Eur. J. Mineral. 22, 837–854.
Neiva, A.M.R., Silva, P.B., Corfu, F., Ramos, J.M.F., 2011. Sequential melting and fractional crystallization: granites from Guarda-Sabugal area, central Portugal. Chem. Erde 71, 227–245.
Neiva, A.M.R., Silva, P.B., Ramos, J.M.F., 2012. Geochemistry of granitic aplite-pegmatite veins and sills and their minerals from the Sabugal area, central Portugal. Neues Jahrb. Mineral. Abh. 189 (1), 49–74.
Neiva, A.M.R., Silva, M.M.V.G., Gomes, M.E.P., 2007. Crystal chemistry of tourmaline from Variscan granites, associated tin-tungsten and gold deposits, and associated metamorphic and metasomatic rocks from northern Portugal. Neues Jahrb. Mineral. Abh. 184, 45–76.
Pal, D.C., Biswajit, M., Bernhardt, H.J., 2007. Mineralogy and geochemistry of pegmatite-hosted Sn-, Ta–Nb- and Zr–Hf-bearing minerals from the southeastern part of the Bastar-Malkangiri pegmatite belt, Central India. Ore Geol. Rev. 30, 30–55.
Peccerillo, A., Pinarelli, L., Del Moro, A.B., Rotura, A., 1994. Interaction between mafic and salic magmas in granitoids plutons as inferred from geochemical and Sr–Nd isotopic study of enclaves and host granitoids from Cima d'Aste, Southern Alps, Italy. Period. Mineraol. 63, 93–111.
Pirard, C., Hatert, F., Fransolet, A.M., 2007. Alteration sequences of aluminium phosphates from Montebras pegmatite, Massif Central, France. In: Martins, T., Vieira, R. (Eds.), Granitic Pegmatites: The State of the Art, Memórias n° 8, Porto, Portugal, pp. 74–75.
Ramos, J.M.F., Silva, P.B., Neiva, A.M.R., Gomes, M.E.P., 2006. Geochemical evolution of LCT pegmatites from the central region of Portugal towards lepidolitic enrichment. In: Mirão, J., Balbino, A. (Eds.), Proceedings from VII National Geological Congress. Estremoz, Portugal, pp. 1193–1198 (in Portuguese).
Rieder, M., Cavazzini, G., D'Yakonov, Yu.S., Frank-Kamenetskii, V.A., Gottardi, G., Guggenheim, S., Koval, P.V., Müller, G., Neiva, A.M.R., Radoslovich, E.W., Robert, J.-L., Sassi, F.P., Takeda, H., Weiss, Z., Wones, D.R., 1999. Nomenclature of the micas. Mineral. Mag. 63, 267–279.
Schärer, U., 1984. The effect of initial ^{230}Th disequilibrium on young U–Pb ages: the Makalu case, Himalaya. Earth Planet. Sci. Lett. 67, 191–204.
Stacey, J.S., Kramers, J.D., 1975. Approximation of terrestrial lead isotope evolution by a two-stage model. Earth Planet. Sci. Lett. 34, 207–226.
Taylor, S.R., McLennan, S.M., 1985. The Continental Crust: Its Composition and Evolution. Blackwell Scientific Publ., Oxford, p. 311.
Tindle, A.G., Breaks, F.W., 2000. Columbite-tantalite mineral chemistry for rare-element granitic pegmatites: Separation Lake area, NW Ontario, Canada. Mineral. Petrol. 70, 165–198.
Tischendorf, G., Gottesmann, B., Förster, H.-J., Trumbull, R.B., 1997. On Li-bearing micas: estimating Li from electron microprobe analyses and an improved diagram from graphical representation. Mineral. Mag. 61, 809–834.
Vieira, R., 2010. Aplitopegmatitos com Elementos Raros da Região entre Almendra (V. N. de Foz-Côa) e Barca d'Alva (Figueira de Castelo Rodrigo). Campo Aplitopegmatítico da Fregeneda-Almendra. Unpublished PhD. Thesis. Porto University, Portugal, p. 192.
Wise, M.A., Černý, P., 1990. Primary compositional range and alteration trends of microlite from the Yellowknife pegmatite field, Northwest Territories. Mineral. Petrol. 43, 83–98.